

A Fast Block Low-Rank Dense Solver with Applications to Finite-Element Matrices

AmirHossein Aminfar^{a,1,*}, Sivaram Ambikasaran^{b,2}, Eric Darve^{c,1}

^a496 Lomita Mall, Room 104, Stanford, CA, 94305

^bWarren Weaver Hall, Room-1105A, 251, Mercer Street, New York, NY 10012

^c496 Lomita Mall, Room 209, Stanford, CA, 94305

Abstract

This article presents a fast solver for the dense “frontal” matrices that arise from the multi-frontal sparse elimination process of 2D and 3D elliptic PDEs. The solver relies on the fact that these matrices can be efficiently represented as a hierarchically off-diagonal low-rank (HODLR) matrix. To construct the low-rank approximation of the off-diagonal blocks, we propose a new pseudo-skeleton scheme, the boundary distance low-rank approximation, that picks rows and columns based on the location of their corresponding vertices in the sparse matrix graph. We also explore a variety of other low-rank approximation methods such as the adaptive cross approximation (ACA) and Chebyshev interpolation for the low-rank approximation of the off-diagonal blocks. Using the HODLR direct solver as a preconditioner (with a low tolerance), we can reach machine accuracy with a simple fixed point iterative scheme much faster than a conventional LU solver. Numerical benchmarks are provided for 2D and 3D finite element matrices that arise from a wide range of applications.

Keywords: Fast direct solvers, Iterative solvers, Numerical linear algebra, Hierarchically off-diagonal low-rank matrices, Multi-frontal elimination, Adaptive cross approximation.

1. Introduction

In many engineering applications, solving large finite element systems is of great significance. Consider the system

$$Ax = b$$

arising from the finite element discretization of an elliptic PDE, where $A \in \mathbb{R}^{N \times N}$ is a sparse matrix with a symmetric pattern. In many practical applications, the matrix A might be ill-conditioned and thus, challenging for iterative methods. On the other hand, conventional direct solver algorithms, while being robust in handling ill-conditioned matrices, are computationally expensive ($\mathcal{O}(N^{1.5})$ for 2D meshes and $\mathcal{O}(N^2)$ for 3D meshes). Since one of the main bottlenecks in the direct multi-frontal solve process is the high computational cost of solving dense frontal matrices, we mainly focus on solving these matrices in this article. Our goal is to build an iterative solver, which utilizes a fast direct solver

*Corresponding author. +1 650-644-7624

Email address: aminfar@stanford.edu (AmirHossein Aminfar)

¹Mechanical Engineering Department, Stanford University

²Courant Institute of Mathematical Sciences, New York University

as a preconditioner for the dense frontal matrices. The direct solver in this scheme acts as an extremely good pre-conditioner (the solver converges after approximately 10 iterations). This approach combines the advantages of the iterative and direct solve algorithms, i.e., it is fast, accurate and robust in handling ill-conditioned matrices.

To be consistent with our previous work, we adopt the notations used in [3]. We should also mention that ‘ n ’ refers to the size of dense matrices and ‘ N ’ refers to the size of sparse matrices (e.g., number of degrees of freedom in a finite-element mesh).

In the next section, we review the previous literature on both dense structured solvers and sparse multi-frontal solvers. We then introduce a simple iterative solver scheme in Section 3 and a hierarchical off-diagonal low-rank (from now on abbreviated as HODLR) direct solver in Section 4. In Section 5, we introduce the boundary distance low-rank (BDLR) algorithm as a robust low-rank approximation scheme for representing the off-diagonal blocks of the frontal matrices. Section 6 discusses the application of the iterative solver with a fast HODLR direct solver preconditioner to the sparse multi-frontal solve process and demonstrates the solver for a variety of 2D and 3D meshes. We also show an application in combination with the FETI-DP method [16], which is a family of domain decomposition algorithms to accelerate finite-element analysis on parallel computers. We present the results and numerical benchmarks in Section 7.

2. Previous Work

2.1. Fast Direct Solvers for Dense Hierarchical Matrices

Hierarchical matrices are data sparse representation of a certain class of dense matrices. This representation relies on the fact that these matrices can be sub-divided into a hierarchy of smaller block matrices, and certain sub-blocks (based on the admissibility criterion) can be efficiently represented as a low-rank matrix. We refer the readers to [21, 25, 20, 22, 10, 13, 11] for more details. These matrices were introduced in the context of integral equations [21, 25] arising out of elliptic partial differential equations and potential theory. Subsequently, it has also been observed that dense matrices arising out of boundary integral equations [50, 36], dense fill-ins in finite element matrices [48], radial basis function interpolation [3], kernel density estimation in machine learning, covariance structure in statistic models [14], Bayesian inversion [3, 5, 6], Kalman filtering [38], and Gaussian processes [4], can also be efficiently represented as data-sparse hierarchical matrices. Broadly speaking, these matrices can be grouped into two general categories based on the admissibility criterion: (i) Strong admissibility: sub-block that correspond to the interaction between well-separated clusters are low-rank; (ii) Weak admissibility: sub-block corresponding to non-overlapping interactions are low-rank. Ambikasaran [1] provides a detailed description of these different hierarchical structures.

We review some of the previously developed structured dense solvers for hierarchical matrices and discuss them in relation to our work. Hackbusch [21, 20] introduced the concept of \mathcal{H} -matrices, which are the most general class of hierarchical matrices with the strong admissibility criterion [21, 20, 22, 24, 23, 25, 26, 7, 8, 10]. Contrary to the HODLR matrix structure, in which the off-diagonal blocks are low-rank, in \mathcal{H} -matrices, the off-diagonal blocks are further decomposed into low-rank and full-rank blocks. Thus, the rank can be kept small. In HODLR, we make a single low-rank approximation for the off-diagonal blocks and the rank is larger as a result. Hence, the HODLR structure makes for a much simpler representation and is often used because of its simplicity compared to the \mathcal{H} -matrix

structure. Hackbusch [20] suggests a recursive block low-rank factorization scheme for \mathcal{H} -matrices. This method is based on the idea that all the dense matrix algebra (matrix multiplication and matrix addition) can be replaced by \mathcal{H} -matrix algebra. As a result, the inverse of an \mathcal{H} -matrix can also be approximated as an \mathcal{H} -matrix itself. This results in a computational complexity of $\mathcal{O}(n \log^2(n))$ for an \mathcal{H} -matrix factorization.

We note that the approach in this paper is based on the Woodbury matrix identity. It is therefore different from the algorithm in Hackbusch [20] for example. The latter is based on a block LU factorization, while the Woodbury identity reduces the global solve to block diagonal solves followed by a correction update.

The HODLR matrix structure is the most general off-diagonal low-rank structure with weak admissibility. Solvers for this matrix class have a computational cost of $\mathcal{O}(n \log^2 n)$. In an HODLR matrix, the off-diagonal low-rank bases do not have a nested structure across different levels [3]. The HSS matrix is an HODLR matrix but, in addition, has a nested off-diagonal low-rank structure. Solvers for the HSS matrices have an $\mathcal{O}(n)$ complexity [49, 12].

Martinsson and Rokhlin [41] discuss an $\mathcal{O}(n)$ direct solver for boundary integral equations based on the HSS structure. Their method is based on the fact that for a matrix of rank r , there exists a well-conditioned column operation, which leaves r columns unchanged and sets the remaining columns to zero. Using this idea, they derive a two-sided compressed factorization of the inverse of the HSS matrix. Their generic algorithm requires $\mathcal{O}(n^2)$ operations to construct the inverse. However, they accelerate their algorithm to $\mathcal{O}(n \log^\kappa(n))$ when applied to two-dimensional contour integral equations.

Chandrasekaran et al. [13] present a fast $\mathcal{O}(n)$ direct solver for HSS matrices. In their article, they construct an implicit ULV^H factorization of an HSS matrix, where U and V are unitary matrices, L is a lower triangular matrix and H is the transpose conjugate operator. Their method is based on the fact that for a low-rank representation of the form UBV^H , where U and V are thin matrices with r columns, there exist a unitary transformation Q , in which only the last r rows of QU are nonzero. They use this observation to recursively compress the matrix and solve the linear system of equations. Since this method requires constructing an HSS tree, the authors suggest an algorithm that uses the SVD or the rank revealing QR decomposition, recursively, to construct the HSS tree in $\mathcal{O}(n^2)$ time.

Gillman et al. [18] discuss an $\mathcal{O}(n)$ algorithm for directly solving integral equations in one-dimensional domains. The algorithm relies on applying the Sherman-Morrison-Woodbury formula (see for example [3]) recursively to an HSS tree structure to achieve $\mathcal{O}(r^2n)$ solve complexity, where r is the rank of the off diagonal blocks in the HSS matrix. They also describe an $\mathcal{O}(r^2n)$ algorithm for constructing an HSS representation of the matrix resulting from a Nyström discretization of a boundary integral equation.

Ho and Greengard [31] present a fast direct solver for HSS matrices. They use the interpolative decomposition (ID) (see for example [32]) algorithm to compress the off-diagonal matrix blocks. This algorithm has a computational complexity of $\mathcal{O}(mn \log r + r^2n)$ for a matrix $K \in \mathbb{R}^{m \times n}$. After obtaining the hierarchical matrix compression of the original dense matrix, new variables and equations are introduced into the system of equations. Finally, all equations are assembled into an extended sparse matrix and a conventional sparse solver is used to factorize the sparse matrix. This method has a computational complexity of $\mathcal{O}(n)$ for both the pre-computation and solution phases for boundary integral equations in 2D, while in 3D, these phases cost $\mathcal{O}(n^{1.5})$ and $\mathcal{O}(n \log(n))$ respectively.

Kong et al. [35] have developed an $\mathcal{O}(n^2)$ dense solver for HODLR matrices. Similar to [41], they accelerate their algorithm to $\mathcal{O}(n \log^2(n))$, when applied to boundary integral equations. Their method uses the Sherman-Morrison-Woodbury formula to construct a

one-sided hierarchical factorization of the inverse of these matrices, in which each factor is a block diagonal matrix. The low-rank approximation scheme in their paper is based on the rank revealing QR algorithm. The authors use the pivoted Gram-Schmidt algorithm to obtain r orthogonal basis vectors for the low-rank matrix in question. For a matrix $K \in \mathbb{R}^{m \times n}$ with rank r , this low-rank approximation scheme requires $\mathcal{O}(mnr)$ operations. Then, they use a randomized algorithm from [47] to accelerate their low-rank approximation scheme. This accelerated low-rank approximation algorithm costs $\mathcal{O}(mn \log(l + lnr))$ in the general case where $r < l < \min(m, n)$.

Ambikasaran and Darve [3] present an $\mathcal{O}(n \log^2(n))$ solver for HODLR matrices and an $\mathcal{O}(n \log(n))$ solver for p-HSS matrices. This approach differs from the approach mentioned in [35] in the fact that, while [35] constructs the inverse, [3] constructs a factorization of the matrix. Each factor in this factorization scheme is a block diagonal matrix with each block being a low-rank perturbation of the identity matrix. The authors then use the Sherman-Morrison-Woodbury formula to invert each block in the block diagonal factors. The article uses the Chebyshev low-rank approximation scheme to factorize the off-diagonal blocks.

As mentioned above, solvers for the HSS matrix structure have the lowest computational complexity — $\mathcal{O}(r^2n)$, r being the rank of approximation — among other hierarchically off-diagonal low-rank matrix structures. Though the HSS structure is attractive, constructing the HSS tree is expensive, typically scaling as $\mathcal{O}(n^2)$ for a $n \times n$ matrix [12, 49]. On the other hand, even though the computational complexity of solvers for the HODLR matrix structure scale as $\mathcal{O}(r^2n \log^2 n)$, the HODLR tree can be constructed in $\mathcal{O}(rn \log(n))$ complexity, i.e., the overall complexity (low-rank assembly + solve) of HODLR solvers is $\mathcal{O}(n \log^2 n)$, while the overall complexity of HSS solvers is typically $\mathcal{O}(n^2)$.

A point worth mentioning is that the solver discussed in the current article relies on purely algebraic technique (instead of analytic or geometry based techniques) to construct the low-rank approximation of the off-diagonal blocks. Analytic low-rank approximation techniques like the Chebyshev low-rank approximation, multipole expansions, etc., are only applicable when the matrix definition involves an analytical kernel function. Some geometry-based techniques, for instance interpolative decomposition, rely on a priori picking a suitable set of “proxy points/surfaces” to represent the matrix. These techniques cannot be used for a black-box solver, where the matrix is known only algebraically (i.e., we only know the numerical values of its entries). To circumvent these issues, in this article, we propose a boundary distance low-rank approximation (from now on abbreviated as BDLR), which relies on the underlying sparse matrix graph to choose the desired rows and columns in constructing a low-rank representation. We also explore the adaptive cross approximation algorithm [43] (from now on abbreviated as ACA), which is also a purely algebraic scheme to construct low-rank approximations of the off-diagonal blocks. However, ACA failed to produce satisfactory results (large error) in several of our benchmarks.

Due to its black-box nature, the solver can handle a wide range of dense matrices arising from boundary integral equations, covariance matrices in statistics, frontal matrices arising in the context of finite-element matrices, etc. Table 1 summarizes the dense solver algorithms mentioned above.

2.2. Fast Direct Solvers for Sparse Matrices

As mentioned in Section 2.1, we are interested in accelerating the direct solve process for finite-element matrices. In this article, we focus on the finite-element discretization of elliptic PDEs. One common way of factorizing such matrices is using the sparse Cholesky factorization. The efficiency of this algorithm strongly depends on the ordering of mesh

Article	Matrix Class	Factorization	Application
Hackbusch [21, 20]	\mathcal{H}	Recursive block factorization of the matrix	BEM integral operators
Martinsson and Rokhlin [41]	HSS	Two sided compressed factorization of the inverse	2D boundary integral equations
Chandrasekaran et al. [13]	HSS	ULV^H factorization of the matrix	Radial basis function matrices
Gillman et al. [18]	HSS	Data sparse factorization of the inverse	1D integral equations with Nyström discretization
Ho and Green-gard [31]	HSS	Factorization of the extended sparse system	2D and 3D boundary integral equations
Kong et al. [35]	HODLR	One sided hierarchical factorization of the inverse	Boundary integral equations
Ambikasaran and Darve [3]	HODLR, p-HSS	Block-diagonal factorization of the matrix	Interpolation using radial basis functions
This article	HODLR	Recursive block LU factorization of the matrix	Finite-element matrices

Table 1: Summary of fast dense structured solvers.

nodes [45]. Sparse Cholesky factorization takes $\mathcal{O}(N^2)$ flops in 2D with a typical row-wise or column-wise mesh ordering, where N is the number of degrees of freedom [48]. The most efficient method for solving such matrices is the multi-frontal method with nested dissection, which takes $\mathcal{O}(N^{1.5})$ flops for two-dimensional and $\mathcal{O}(N^2)$ for three dimensional meshes [45].

The multi-frontal method was originally introduced by Duff & Reid [15] as an extension to the frontal method of Irons [33]. In this algorithm, the overall factorization is done by factorizing smaller dense frontal matrices [39]. For each node or super-node in the elimination tree, the frontal matrix is obtained using an update process called the “extend-add” process, which involves updates from the previously eliminated nodes.

There have been some recent efforts to reduce the computational cost of the multi-frontal method with nested dissection. Xia et al. [48] observed that frontal and update matrices in the multi-frontal elimination process can be approximated with hierarchically semi-separable (HSS) matrices. The authors develop a structured extend-add process to facilitate the formation of the frontal matrices using the HSS structure. Next, they perform a structured dense Cholesky factorization on the obtained frontal matrix. The authors use the algorithm in [12] to compute the explicit factorizations of HSS matrices. Using this procedure, they are able to achieve nearly linear time complexity. However, only regular well shaped meshes are considered in the article. Schmitz et al. [45] extend the approach of [48] to a more general setting of unstructured and adaptive grids.

Martinsson [40] uses a spiral elimination approach along with HSS compression of Schur complements to achieve $\mathcal{O}(N \log^2 N)$ time complexity. This approach requires a mesh that can be partitioned into concentric annuli.

The approach presented here is based on the multi-frontal method [39]. It doesn’t require constructing and maintaining HSS trees and can be applied to any mesh structure. Our

method is based on the observation that the frontal matrices obtained during the multi-frontal elimination process have an HODLR structure. This observation was also made by [48]. In order to factorize (eliminate) these frontal matrices, we present a dense HODLR structured solver that scales as $\mathcal{O}(n \log^2 n)$ for an $n \times n$ matrix. We will benchmark the structured elimination (solve) process for frontal matrices corresponding to separators at various levels of the sparse elimination tree, for many different types of sparse matrices.

3. An Iterative Solver with Direct Solver Preconditioning

In this paper, we investigated using a fast HODLR direct solver as a preconditioner to an iterative scheme. In this case, we used a relatively low accuracy for the direct solver. As soon as $\rho(I - A_{\text{HODLR}}^{-1}A) \ll 1$ (where A is the matrix, A_{HODLR}^{-1} corresponds to the approximate solve using the fast direct solver, ρ denotes the spectral radius), we can get convergence with a few iterations using any classical iterative scheme, e.g.:

$$x_{n+1} = x_n + A_{\text{HODLR}}^{-1}(b - Ax_n) \quad (1)$$

We will show that this approach is much faster than both a conventional LU solver and a high accuracy direct HODLR solver. We should also mention that this preconditioning method can be applied to more sophisticated iterative solvers (conjugate gradient (CG) [30], generalized minimal residual (GMRES) [44], etc). However, we only investigated the fixed point iterative scheme [Eq. (1)] in this article.

4. A Fast Direct Solver for HODLR Matrices

4.1. HODLR Matrices

A HODLR matrix has low-rank off-diagonal blocks at multiple levels. As described in [3], a 2-level HODLR matrix, $K \in \mathbb{R}^{n \times n}$, can be written as shown in Eq. (2):

$$K = \begin{bmatrix} K_1^{(1)} & U_1^{(1)}V_{1,2}^{(1)T} \\ U_2^{(1)}V_{2,1}^{(1)T} & K_2^{(1)} \end{bmatrix} = \begin{bmatrix} \begin{bmatrix} K_1^{(2)} & U_1^{(2)}V_{1,2}^{(2)T} \\ U_2^{(2)}V_{2,1}^{(2)T} & K_2^{(2)} \end{bmatrix} & U_1^{(1)}V_{1,2}^{(1)T} \\ U_2^{(1)}V_{2,1}^{(1)T} & \begin{bmatrix} K_3^{(2)} & U_3^{(2)T}V_{3,4}^{(2)T} \\ U_4^{(2)}V_{4,3}^{(2)T} & K_4^{(2)} \end{bmatrix} \end{bmatrix} \quad (2)$$

where for a p -level HODLR matrix, $K_i^{(p)} \in \mathbb{R}^{n/2^p \times n/2^p}$, $U_{2i-1}^{(p)}, U_{2i}^{(p)}, V_{2i-1,2i}^{(p)}, V_{2i,2i-1}^{(p)} \in \mathbb{R}^{n/2^p \times r}$ and $r \ll n$. Further nested compression of the off-diagonal blocks will lead to HSS structures [3].

4.2. Solver Derivation and Algorithm

Contrary to the method introduced by Hackbusch [21] which utilizes sequential block LU factorization, the HODLR direct solve algorithm presented in this section is based on the Woodbury matrix identity (see for example [27, 3]). Although we don't use the formula explicitly, we perform the exact same operations. Looking at Equation (4), our method assumes that both diagonal blocks are non singular and factorizes them independently. However, Hackbusch [21] only assumes that top diagonal block is invertible and factorizes the top diagonal block first. He then constructs the remaining Schur complement and continues on with the factorization. In comparing the two methods, one can see that

because of the independent factorization of the diagonal blocks, the method presented in this section is better suited to parallel implementations.

Consider the following linear equation:

$$Kx = F \quad (3)$$

where $K \in \mathbb{R}^{n \times n}$ is an HODLR matrix and $x, F \in \mathbb{R}^{n \times s}$. Now let's write K as a one-level HODLR matrix and rewrite Eq. (3) :

$$K = \begin{bmatrix} K_1^{(1)} & U_1^{(1)} V_{1,2}^{(1)T} \\ U_2^{(1)} V_{2,1}^{(1)T} & K_2^{(1)} \end{bmatrix} \begin{bmatrix} x_1^{(1)} \\ x_2^{(1)} \end{bmatrix} = \begin{bmatrix} F_1^{(1)} \\ F_2^{(1)} \end{bmatrix} \quad (4)$$

where $x_i^{(1)}, F_i^{(1)} \in \mathbb{R}^{(\frac{n}{2} \times s)}$. We now introduce two new variables $y_1^{(1)}$ and $y_2^{(1)}$:

$$y_1^{(1)} = V_{2,1}^{(1)T} x_1^{(1)} \quad (5)$$

$$y_2^{(1)} = V_{1,2}^{(1)T} x_2^{(1)} \quad (6)$$

Rearranging (4), we have:

$$\underbrace{\begin{bmatrix} K_1^{(1)} & 0 & 0 & U_1^{(1)} \\ 0 & K_2^{(1)} & U_2^{(1)} & 0 \\ -V_{2,1}^{(1)T} & 0 & I & 0 \\ 0 & -V_{1,2}^{(1)T} & 0 & I \end{bmatrix}}_{\widehat{K}} \underbrace{\begin{bmatrix} x_1^{(1)} \\ x_2^{(1)} \\ y_1^{(1)} \\ y_2^{(1)} \end{bmatrix}}_{\widehat{x}} = \underbrace{\begin{bmatrix} F_1^{(1)} \\ F_2^{(1)} \\ 0 \\ 0 \end{bmatrix}}_{\widehat{F}} \quad (7)$$

We now factorize the top diagonal block of \widehat{K} which consists of $K_1^{(1)}$ and $K_2^{(1)}$. Since this subblock of \widehat{K} is a block diagonal matrix, this means that we only need to factorize $K_1^{(1)}$ and $K_2^{(1)}$. After eliminating the top off diagonal block, we are left with the Schur complement:

$$S^{(1)} = \begin{bmatrix} I & V_{2,1}^{(1)T} K_1^{(1)-1} U_1^{(1)} \\ V_{1,2}^{(1)T} K_2^{(1)-1} U_2^{(1)} & I \end{bmatrix} \quad (8)$$

All we have to do now, is to solve the Schur complement:

$$S^{(1)} \begin{bmatrix} y_1^{(1)} \\ y_2^{(1)} \end{bmatrix} = \begin{bmatrix} V_{2,1}^{(1)T} K_1^{(1)-1} F_1^{(1)} \\ V_{1,2}^{(1)T} K_2^{(1)-1} F_2^{(1)} \end{bmatrix} \quad (9)$$

At this point, we can write $x_1^{(1)}$ and $x_2^{(1)}$ in terms of $K_1^{(1)-1}$ and $K_2^{(1)-1}$:

$$\begin{bmatrix} x_1^{(1)} \\ x_2^{(1)} \end{bmatrix} = \begin{bmatrix} K_1^{(1)-1} & 0 \\ 0 & K_2^{(1)-1} \end{bmatrix} \begin{bmatrix} F_1^{(1)} - U_1^{(1)} y_2^{(1)} \\ F_2^{(1)} - U_2^{(1)} y_1^{(1)} \end{bmatrix} \quad (10)$$

Since, both $K_1^{(1)}$ and $K_2^{(1)}$ are HODLR matrices, we can apply the same procedure for factorizing them. Thus, we have arrived at a recursive algorithm for solving (7). The factorization step corresponds to the computation and storage of all the terms that are independent of the right hand side (i.e., the Schur complements at all levels).

4.3. Algorithm Summary

We now summarize the recursive HODLR direct solver algorithm. For a matrix such as $K \in \mathbb{R}^{n \times n}$, we have to carry out the following procedure at each recursion step (p) for all $1 \leq i \leq 2^p$:

1. Find the low-rank approximation of the off-diagonal blocks $(U_{2i-1}^{(p)}, U_{2i}^{(p)}, V_{2i-1,2i}^{(p)}, V_{2i,2i-1}^{(p)})$.
2. Recursively solve the following equations with multiple right hand sides:

$$\begin{bmatrix} d_{2i-1}^{(p)} & c_{2i-1}^{(p)} \end{bmatrix} = K_{2i-1}^{(p)-1} \begin{bmatrix} U_{2i-1}^{(p)} & F_{2i-1}^{(p)} \end{bmatrix} \quad (11)$$

$$\begin{bmatrix} d_{2i}^{(p)} & c_{2i}^{(p)} \end{bmatrix} = K_{2i}^{(p)-1} \begin{bmatrix} U_{2i}^{(p)} & F_{2i}^{(p)} \end{bmatrix} \quad (12)$$

3. Obtain $y_{2i-1}^{(p)}, y_{2i}^{(p)}$ using Eq. (8) and Eq. (9):

$$\begin{bmatrix} I & V_{2i,2i-1}^{(p)T} d_{2i-1}^{(p)} \\ V_{2i-1,2i}^{(p)T} d_{2i}^{(p)} & I \end{bmatrix} \begin{bmatrix} y_{2i-1}^{(p)} \\ y_{2i}^{(p)} \end{bmatrix} = \begin{bmatrix} V_{2i,2i-1}^{(p)T} c_{2i-1}^{(p)} \\ V_{2i-1,2i}^{(p)T} c_{2i}^{(p)} \end{bmatrix} \quad (13)$$

4. Obtain $x_{2i-1}^{(p)}, x_{2i}^{(p)}$ using:

$$x_1^{(p)} = c_{2i-1}^{(p)} - d_{2i-1}^{(p)} y_{2i}^{(p)} \quad (14)$$

$$x_2^{(p)} = c_{2i}^{(p)} - d_{2i}^{(p)} y_{2i-1}^{(p)} \quad (15)$$

4.4. Solver Computational Cost

Assuming we use a fast ($\mathcal{O}(n)$) low-rank approximation scheme, the cost of constructing and storing an HODLR matrix is $\mathcal{O}(nr \log(n))$ [3], where r is the rank of approximation. Further, we assume that the rank of approximation at all levels of the HODLR matrix is equal to r . Looking at the procedure described in Section 4.3, we can write the following:

$$C^{(p)}(r, s, n) = 2C^{(p+1)}\left(r, s + r, \frac{n}{2}\right) + \mathcal{O}(nr^2) + \mathcal{O}(nsr) \quad (16)$$

where $C^{(p)}(r, s, n)$ is the computational cost associated with solving an $n \times n$ HODLR matrix at level p with s right hand sides and off-diagonal blocks of rank r . Eq. (16) suggests that the cost of solving a HODLR matrix at level p with s right hand sides is made up of three contributions. The first contribution is associated with solving the two diagonal blocks at the lower level ($p + 1$) with $s + r$ right hand sides. The second contribution comes from constructing the update matrix $S^{(p)}$ [Eq. (8)] and the third contribution is the cost of constructing the right hand side of Eq. (9). Writing Eq. (16) as a sum, we have:

$$C^{(0)}(r, s, n) = \sum_{p=1}^{\log\left(\frac{n}{r}\right)} \mathcal{O}(pnr^2 + nsr) = \mathcal{O}(r^2 n \log^2(n)) \quad (17)$$

5. Low-Rank Approximation Schemes

In this section, we discuss the various low-rank approximations schemes used for obtaining a low-rank representation of the off-diagonal blocks of our HODLR matrices. Although a variety of low-rank approximation algorithms (SVD, rank revealing LU, rank revealing QR, etc) are available, we require a scheme that has a computational cost of $\mathcal{O}(rn)$ where r is the rank of approximation and n is the size of the matrix. This requirement limits our choices to methods like Chebyshev (Section 5.1), partial pivoting ACA (Section 5.2) and the pseudo-skeleton low-rank approximation algorithm (Section 5.3). Each of these methods has certain drawbacks:

- The Chebyshev low-rank approximation algorithm is only suited to cases dealing with interaction of points via smooth kernels.
- The partial pivoting ACA algorithm does a good job when all rows and columns have fairly the same importance when constructing the low-rank approximation. However, in cases where certain rows or columns play a special role and are critical to include in the low-rank approximation, ACA often fails to properly identify them. As a result, in several of the benchmarks presented here, the low-rank approximation was very inaccurate.
- The accuracy of the pseudo-skeleton low-rank approximation scheme strongly depends on the method used for selecting rows and columns.

In order to construct a fast and robust low-rank approximation scheme, we introduce an algorithm for selecting rows and columns in the pseudo-skeleton low-rank approximation algorithm. We call this new method the boundary distance low-rank approximation scheme (BDLR). We primarily used the BDLR method for our benchmarks and demonstrate other low-rank approximation schemes such as ACA, mostly for comparison purposes.

5.1. Chebyshev Low-Rank Approximation

The Chebyshev low-rank approximation scheme is only presented here for comparison purposes. For detailed explanations of this algorithm, see for example [17] and [3]. One of the main differences between this algorithm and the ACA algorithm is that the rank of approximation is user-determined and fixed among various levels in the hierarchy. Hence, we can verify the convergence of our solve algorithm by plotting the solver error vs. rank of approximation.

5.2. ACA Low-Rank Approximation

We use the partial pivoting ACA algorithm [43] to perform some simple benchmarks on radial basis function interaction matrices in 1D. Although ACA is a relatively fast low-rank approximation algorithm, it is not a very robust low-rank approximation method especially in cases where the matrix corresponds to a 2D or a 3D geometry and needs to be fine tuned to achieve a desired accuracy. We use the ACA algorithm with partial pivoting as described by Rjasanow [43]. This algorithm is an algebraic low-rank approximation scheme and works on any dense matrix without any prior knowledge of the matrix. Unlike the Chebyshev low-rank approximation scheme, the rank of approximation in this algorithm is dynamically determined at each level of solve. The ACA algorithm has a cost of $\mathcal{O}(r(m+n))$, for a matrix $A \in \mathbb{R}^{m \times n}$ [43], where r is the rank of approximation.

One important factor to note about the ACA algorithm is the stopping criterion. We use the same stopping criterion mentioned in [43]. As suggested by Rjasanow [43], a good stopping criterion is when the following holds for iteration $k = r$:

$$\|w_r\|_F \|v_r\|_F \leq \epsilon_{ACA} \|S_r\|_F \quad (18)$$

where w_r and v_r are the r th low-rank approximate matrices, S_r is the approximate matrix at the r th iteration, and ϵ_{ACA} is an arbitrary tolerance chosen by the user.

5.3. Pseudo-Skeleton and Boundary Distance Low-Rank Approximation

In order to construct a fast and accurate solver, we need an accurate and robust method to construct low-rank approximations. As mentioned before, ACA is not very robust and only works when the choice of row/column is “easy” and Chebyshev only works for smooth kernels. As we will show, BDLR is very robust and leads to accurate low-rank approximations. It works well in problems where the matrix can be loosely related to a Green’s function. In that case, large entries correspond to points close in space, which we associate as a simplification to nodes in the graph that are connected by few edges. Although this is a simple heuristic, it worked very well in our examples and allowed us to efficiently form accurate low-rank approximations.

The BDLR algorithm is a row and column selection algorithm in the pseudo-skeleton low-rank approximation scheme. The pseudo-skeleton algorithm allows us to construct a low-rank approximation of a matrix by choosing a subset of rows and columns of that matrix. As mentioned in [19], for a low-rank matrix A , if we pick a set of row indices ($i \in I = \{i_1, \dots, i_r\}$) and a set of column indices ($j \in J = \{j_1, \dots, j_r\}$) and define matrices C and R such that :

$$R = A(I, :) \quad (19)$$

$$C = A(:, J) \quad (20)$$

Then, we can approximate A to be :

$$A \approx C \hat{A}^{-1} R \quad (21)$$

where $\hat{A} = A(I, J)$. In some cases, the Moore-Penrose pseudo-inverse is needed for \hat{A}^{-1} . In order to achieve a certain accuracy, one can increase the number of chosen rows and columns until the desired accuracy is reached. To monitor the error in the scheme, we pick rows and columns that are not in the set of rows and columns already chosen for low-rank approximation. We then monitor the relative Frobenius norm error on these rows and columns and increase the rank of the approximation until the relative Frobenius norm error falls below a certain tolerance.

For a rank r pseudo-skeleton low-rank approximation, the inversion of \hat{A} has a computational cost of $\mathcal{O}(r^3)$. Monitoring the error has a computational cost of $\mathcal{O}(mr + nr - r^2)$ for $A \in \mathbb{R}^{m \times n}$. Thus, this method has an asymptotic complexity of $\mathcal{O}(nr)$.

As mentioned in Section 1, we are predominantly interested in solving dense frontal matrices arising from the multi-frontal elimination process of sparse finite-element matrices. In this case, every frontal matrix has a corresponding sparse matrix, which is a diagonal sub-block of the original finite-element matrix. This sparse matrix describes a graph that has rows and columns of the dense matrix as its vertices and the edges in this graph

describe the connection between these points. We use this graph in constructing the low-rank approximation of the off-diagonal blocks.

Entries in dense matrix blocks that correspond to FEM or BEM applications can be related to the inverse of a Green’s function. The Green’s function is large at short distances and then decays smoothly. We have a similar behavior for our dense blocks. Hence, we want to identify row/column pairs corresponding to large entries. These correspond to nodes in the graph that are close, that is connected by few edges. Therefore we use the distance between a row vertex in the graph and the column vertex set (e.g., if the vertex corresponds to a row, we consider the distance to the set of vertices associated with the columns, and vice versa) as a good criterion to determine whether to pick a row/column or not.

For a set of row (column) vertices, we define the boundary vertices as the subset of vertices for which there exists an edge in the interaction graph connecting them to a vertex in the column (row) set. Now that we have defined the boundary nodes, we can designate an index d for every vertex in the row (column) set. This index is defined as the distance of a vertex to the vertices in the boundary set. In order to construct the low-rank approximation, we choose rows and columns based on their d index value. That is, we first choose rows (columns) that are in the boundary set ($d = 0$). We then add rows (columns) with a distance of one to the boundary ($d = 1$). We continue adding points based on the d index, until we reach the desired accuracy. Figure 1 shows an illustration of this algorithm.

As mentioned above, calculating the pseudo skeleton low-rank approximation requires us to calculate the pseudo inverse of \hat{A} . For the BDLR algorithm, instead of using the SVD for calculating the pseudo inverse (\hat{A}^{-1}), we use a full pivoting LU factorization, which is slightly cheaper:

$$\hat{A} = P^{-1}LUQ^{-1} \quad (22)$$

where P and Q are permutation matrices. Let r be the rank of \hat{A} . Define \tilde{R} and \tilde{C} as:

$$\tilde{C} = (CQ)(:, 1 : r)(U(1 : r, 1 : r))^{-1} \quad (23)$$

$$\tilde{R} = (L(1 : r, 1 : r))^{-1}(PR)(1 : r, :) \quad (24)$$

where C and R are the subset of columns and rows we have picked using the BDLR scheme. We then have:

$$A \approx \tilde{C} \tilde{R} \quad (25)$$

$(U(1 : r, 1 : r))^{-1}$ and $(L(1 : r, 1 : r))^{-1}$ correspond to lower-triangular solves. The inverse matrices are not explicitly computed.

6. Application for Multi-frontal Solve Process

In this section, we demonstrate how our fast dense solver algorithm can be applied to a sparse multi-frontal solve process. We will not explain the multi-frontal algorithm in detail. For a detailed review of the multi-frontal method see [39]. We applied our fast solver as described in Section 3 to a variety of 2D and 3D finite-element problems. In the 2D case, we investigate the top level frontal matrix of a sparse matrix corresponding to the heat transfer equation in the turbine blade geometry. In this case, we create an artificial separator, which is the outer boundary of the mesh. We do this mainly because conventional 2D separators have a relatively simple geometry and we wanted to test our solver with a more complex separator. For the 3D benchmarks, we investigate frontal matrices at various levels of the sparse matrix elimination tree corresponding to the elasticity equation. Contrary to the

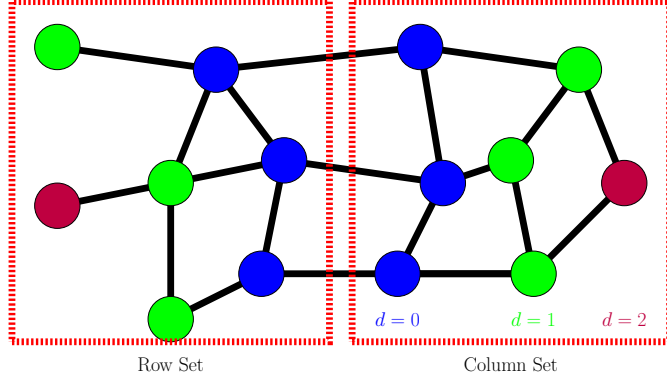


Figure 1: Classification of vertices based on distance from the other set.

2D case, all matrices for the 3D benchmarks are actual frontal matrices that appear in a conventional multi-frontal solver. In our case, we use SCOTCH [42] to do the reordering in the sparse multi-frontal solver.

Our goal is to apply our fast dense solver to the dense frontal matrices obtained in the multi-frontal elimination process of a sparse finite-element matrix, and speed up the algorithm to approximately $\mathcal{O}(N)$. The results shown in this paper can be viewed as a proof of concept of this idea.

6.1. Heat Transfer Problem in a 2D Turbine Blade Geometry

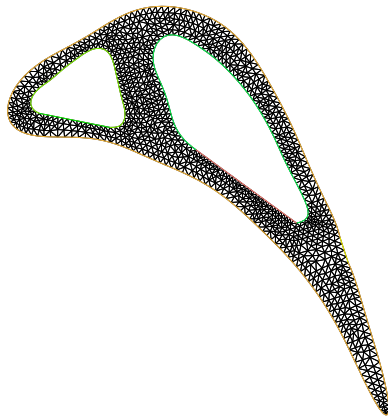
We considered the 2D heat equation with no volumetric heat generation (Equation (26)) in a sample turbine blade geometry shown in Figure 2(a) as described in [46]. This particular blade geometry is similar to the stage-1 high pressure turbine blade design of the NASA E^3 engine [28].

$$\nabla^2 u = 0 \quad (26)$$

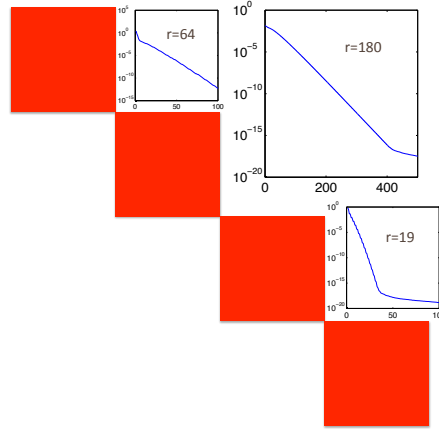
We used Freefem++ [29] to obtain the stiffness matrix corresponding to the finite-element discretization of the above equation on the turbine blade geometry. Since the stiffness matrix is the same regardless of the boundary condition, we used Dirichlet boundary conditions, as the rows and columns corresponding to boundary nodes are more easily identifiable in this case. We create an artificial separator by reordering the rows and columns of the sparse stiffness matrix such that the rows and columns corresponding to the nodes on the boundaries of the mesh are located at the bottom right corner of the matrix. Further, the ordering is such that the rows and columns corresponding to adjacent boundary nodes are grouped together in the matrix. Now, we eliminate the unknowns corresponding to the nodes lying inside the turbine blade:

$$A = \begin{bmatrix} B & V^t \\ V & C \end{bmatrix} = \begin{bmatrix} L_B & 0 \\ VL_B^{-t} & I \end{bmatrix} \begin{bmatrix} I & 0 \\ 0 & C - VB^{-1}V^t \end{bmatrix} \begin{bmatrix} L_B^t & L_B^{-1}V^t \\ 0 & I \end{bmatrix} \quad (27)$$

Here, the matrix block B corresponds to self interaction of all the inner nodes, the blocks V , V^t correspond to the interaction of inner nodes with the boundary nodes, and block C corresponds to the self-interaction of the boundary nodes. As can be seen in Eq. (27), the part of the matrix that remains to be factored is the Schur complement, $C - VB^{-1}V^t$. The main point is that this Schur complement is dense and has the HODLR structure.



(a) FE mesh for the turbine blade geometry



(b) Structure of root separator Schur Complement

Figure 2: a) An unstructured 2D mesh for the turbine blade geometry. b) HODLR structure of the root separator Schur complement of size $\approx 10 \text{ k} \times 10 \text{ k}$. This figure shows the singular value decay of the off-diagonal blocks, where r is the rank of approximation.

Figure 2(b) shows this structure for a Schur complement obtained from the elimination of a mesh with approximately 640k total nodes and 10k nodes on the boundaries. The Schur complement structure clearly shows that the off-diagonal blocks are in fact low-rank and thus, we can use our fast HODLR solver to factorize this matrix.

6.2. Elasticity Equation for a 3D Beam

As mentioned in Section 6, we consider the 3D Navier-Cauchy elastostatics equations with a beam geometry (figure 3):

$$(\lambda + \mu)\nabla(\nabla \cdot \mathbf{u}) + \mu\nabla^2\mathbf{u} + \mathbf{F} = 0 \quad (28)$$

where \mathbf{u} is the displacement vector and λ and μ are Lamé parameters. We use 10-node tetrahedral elements (see for example Section 10.2 of this document³ for example) to discretize the above equation. Figure 3 shows a sample beam geometry. As can be seen, we've considered an unstructured mesh for solving this problem.

6.3. FETI-DP Solver for a 3D Elasticity Problem

Domain decomposition (DD) methods solve a problem by splitting it into several subdomains. Local problems are solved on each subdomain and a global linear system is used to couple these local solutions into a global solution for the entire problem [9]. FETI methods [16, 37] are a family of domain decomposition algorithms with Lagrange multipliers that have been developed for the fast sequential and parallel iterative solution of large-scale systems of equations arising from the finite-element discretization of partial differential equations [16].

In this article, we consider two sparse local FETI-DP matrices arising from the finite-element discretization of an elasticity problem in three dimensions. The first matrix corresponds to solving the elasticity equation with a structured mesh in three dimensions

³<http://www.colorado.edu/engineering/CAS/courses.d/AFEM.d/AFEM.Ch10.d/AFEM.Ch10.pdf>

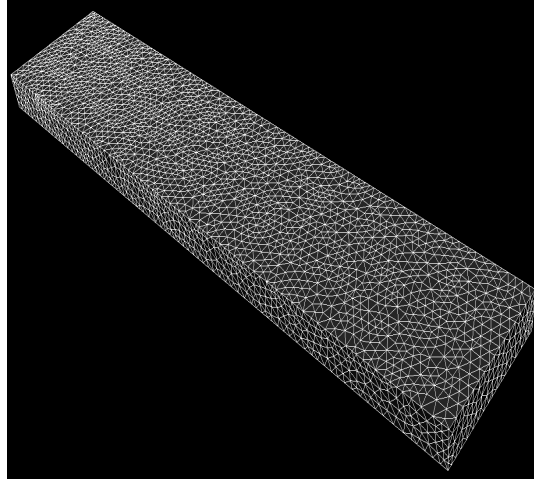
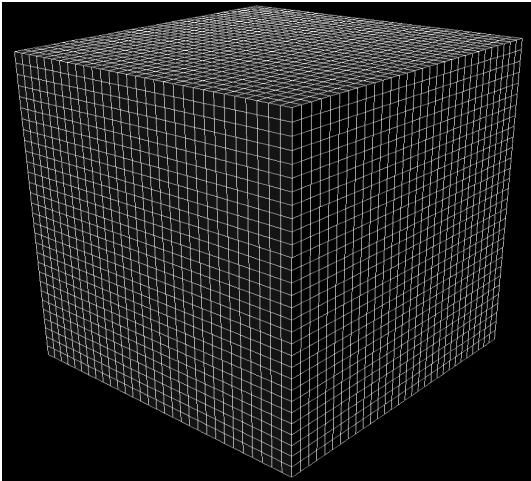
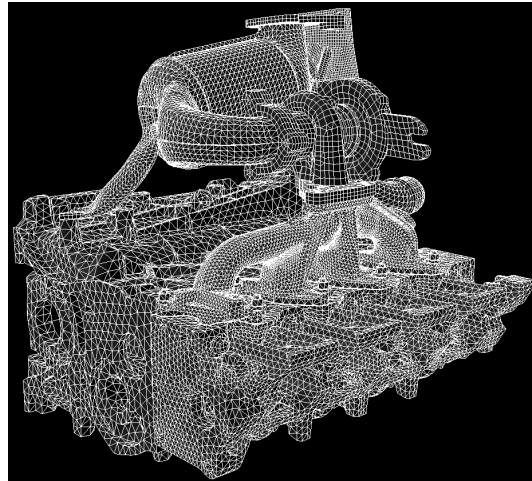


Figure 3: 3D unstructured mesh for the beam problem.



(a) Structured Mesh



(b) Unstructured Mesh

Figure 4: FETI-DP benchmark meshes. Figure (a) shows a structured and figure (b) shows an unstructured 3D FETI-DP mesh.

(figure 4(a)) while the second matrix corresponds to solving the same problem using the geometry of an engine in an unstructured mesh (figure 4(b)). Both matrices have a dimension of $400k \times 400k$ and correspond to the stiffness matrix of one subdomain of a linear elastic 3D solid finite element model (Equation (28)) of their respective geometry. The discretization for the cube geometry uses 8-node (trilinear) hexahedral elements (see for example Section 11.3 of this online document⁴) while the discretization for the engine geometry uses a 10-node tetrahedral elements (see for example Section 10.2 of this document⁵).

7. Numerical Benchmarks

In this section we show some numerical results as well as simple benchmarks of our code.

7.1. Direct Solver for 1D Radial Basis Function Matrices

We first tested our direct HODLR solver (Section 4) on dense matrices arising from the interaction of points lying on a 1D interval, where the interaction can be described by a radial basis function. These benchmarks serve as a validation check for the direct solver code and the asymptotic computational cost of the direct solver algorithm. We also compare the performance of the Chebyshev (Section 5.1) and the partial pivoting ACA (Section 5.2) algorithms as low-rank approximation schemes for the off-diagonal blocks of such matrices.

$1 + d^2$	$\sqrt{1 + d^2}$	$(1 + d^2)^{-1}$	$(1 + d^2)^{-1/2}$	$\exp(-d^2)$	$\exp(-d)$	$\log(1 + d)$	d^{-1}	$d^{-1/2}$	$\log(d)$
1.7×10^4	1.1×10^4	5.8×10^5	5.8×10^4	1.5×10^4	5.4×10^5	4.8×10^7	7.6×10^5	2.5×10^6	3.1×10^6

Table 2: Condition numbers for 1D radial basis function matrices of size $10,000 \times 10,000$. The relatively high condition numbers (e.g., $5 \cdot 10^7$ for $\log(1 + d)$) means that it is difficult to have roundoff errors smaller than about 10^{-9} , unless an iterative refinement or other scheme is used to reduce the error.

In the Chebyshev algorithm, one must specify the desired approximation rank (r), while in the ACA algorithm, the approximation tolerance (ϵ_{ACA}) must be specified as an input to the algorithm. Figure 5 shows the convergence plots for both low-rank approximation methods for various radial basis kernels. As can be seen, both of these algorithms do a good job in approximating the off-diagonal blocks of 1D radial basis function matrices as low-rank products. Moreover, as Figure 5(b) shows, the ACA solver is capable of handling kernels with singularity on the diagonal ($d = 0$). We can also observe that as we decrease the ACA tolerance (ϵ_{ACA} , see Eq. (18)), we arrive at lower errors in our final solution. Table 2 shows the condition numbers for the benchmark matrices. Another point worth mentioning is that in this particular case, the ACA algorithm results in a much lower off-diagonal rank compared to the Chebyshev algorithm for the same solver relative error. Figure 6 shows the off-diagonal ACA rank of various radial basis function matrices. As can be seen in Figures 5 and 6, in order to reach a solve accuracy of 10^{-10} , the ACA algorithm requires a rank of $r \leq 10$, while Chebyshev requires $r \geq 15$.

We have also conducted a comprehensive speed comparison for the two algorithms. Figures 7 shows the results of such comparison. We have compared our fast solver to the partial pivoting LU solver in the Eigen C++ library [34] as a standard dense solver. As shown in the figures, for non singular kernels, both the Chebyshev solver and the ACA

⁴<http://www.colorado.edu/engineering/CAS/courses.d/AFEM.d/AFEM.Ch11.d/AFEM.Ch11.pdf>

⁵<http://www.colorado.edu/engineering/CAS/courses.d/AFEM.d/AFEM.Ch10.d/AFEM.Ch10.pdf>

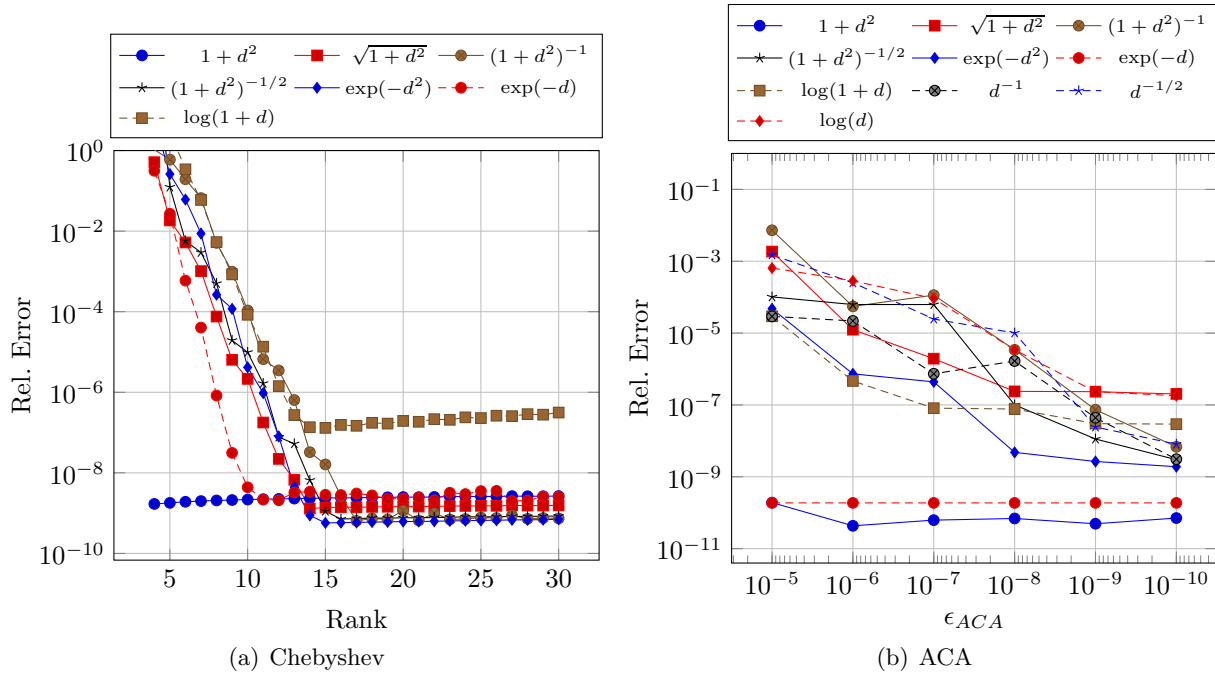


Figure 5: Convergence plots for the solver using Chebyshev and ACA low-rank approximation schemes. These plots show the relative error in the solver for matrices with various radial basis function kernels and size of $10,000 \times 10,000$. The matrices correspond to a uniform point distribution on the interval $[-1, 1]$. The diagonal entries of all the matrices are set to 0. In the legend, d denotes the distance between the points in $[-1, 1]$. See Eq. (18) for the definition of the stopping criterion ϵ_{ACA} .

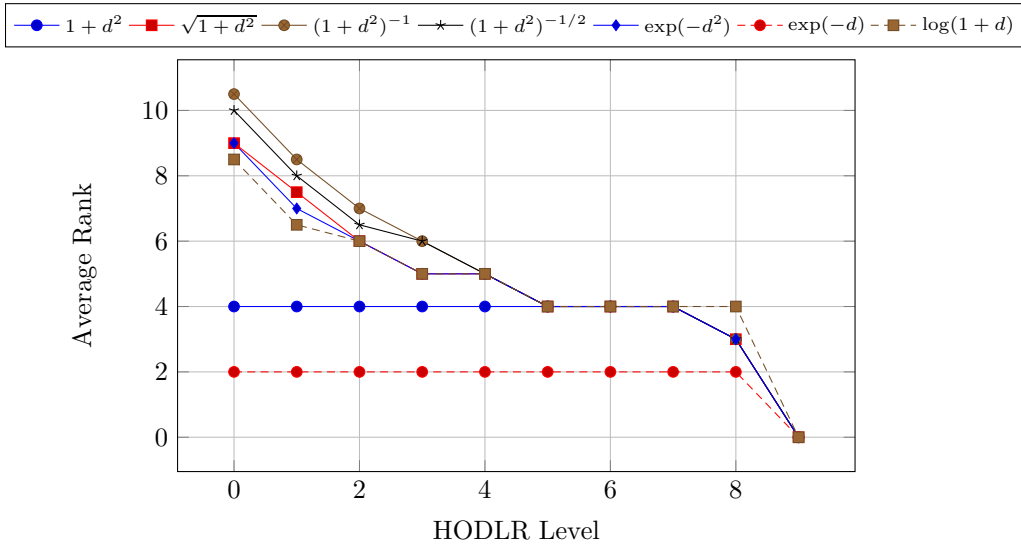


Figure 6: Average off-diagonal ACA rank vs HODLR level. This figure shows the average off-diagonal rank at each level for various radial basis function matrices. Each matrix has a size of $10,000 \times 10,000$ and has been obtained from a uniform point distribution on the interval $[-1, 1]$. The low-rank approximations have been obtained using the partial pivoting ACA algorithm with a tolerance of 10^{-10} ($\epsilon_{ACA} = 10^{-10}$).

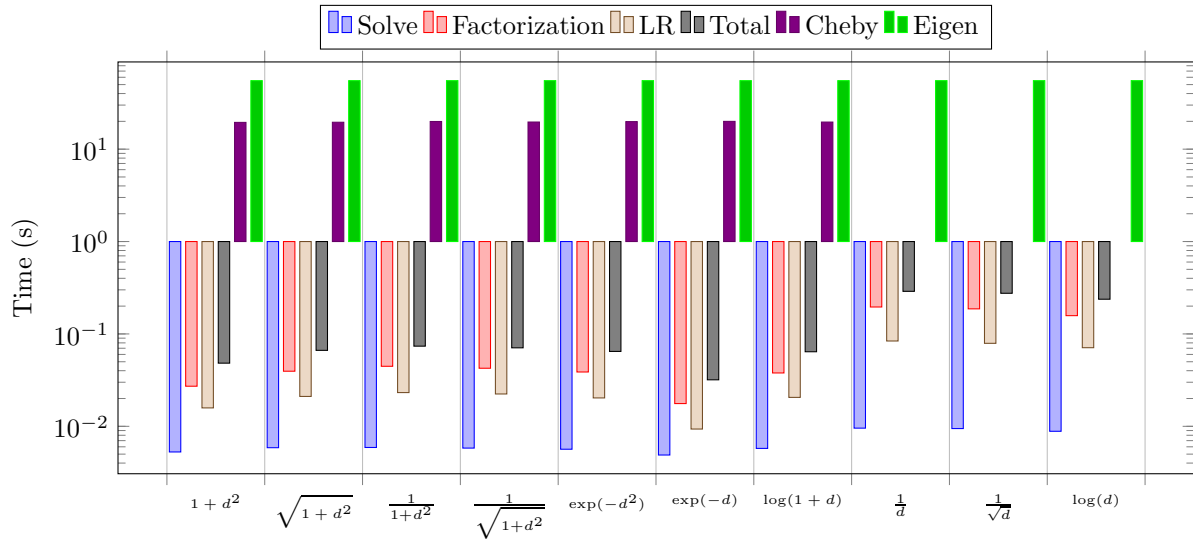


Figure 7: Time taken for the various stages of the HODLR solver with ACA low-rank approximation for $10,000 \times 10,000$ matrices corresponding to various rbf kernels. The matrices correspond to a 1D uniform point distribution on the interval $[-1, 1]$. The diagonal entries of all the matrices are set to 0. The ACA tolerance is $\epsilon_{ACA} = 10^{-10}$. LR is the cost of computing the low-rank approximation of the blocks for the HODLR format using ACA. The CPU time for the HODLR solver with the Chebyshev low-rank approximation and the Eigen LU [34] solver have also been included for comparison purposes. Cheby time denotes the total solve time of the direct HODLR solver with Chebyshev low-rank approximation. The off-diagonal rank for the Chebyshev low-rank approximation was set to $r = 30$. The last few kernels do not have timings for the Chebyshev method since the kernels are singular.

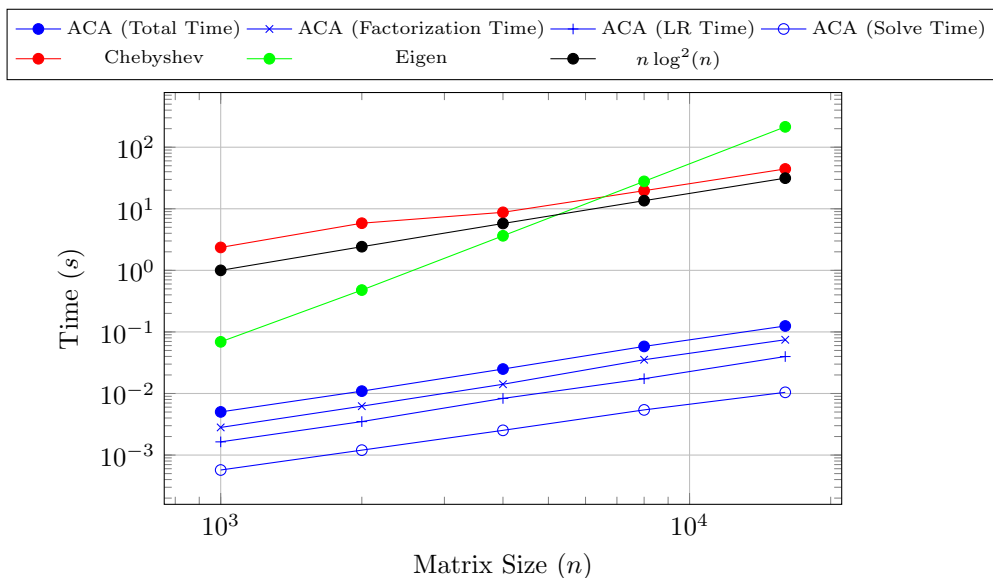


Figure 8: CPU time (seconds) vs. matrix size (n) for matrices defined with the radial basis function kernel $(1 + d^2)^{-1/2}$. Similar plots were obtained for all the kernels shown in Fig. 7 and the trends are similar, in particular the asymptotic growth is $O(n \log^2 n)$. This plot shows the CPU time for a variety of solve methods including Eigen’s partial pivoting LU solver [34], the fast solver with Chebyshev low-rank approximation, and various stages of the fast solver with the ACA scheme. The diagonal entry of all matrices is set to zero. The ACA tolerance (ϵ_{ACA}) for the ACA solver was 10^{-10} and the rank of approximation for the Chebyshev solver was 30. For Chebyshev, the rank is fixed and therefore the computational time grows very closely like $O(n \log^2 n)$. For ACA, the rank varies with n (and the accuracy ϵ) and therefore the asymptotic growth with n is more difficult to determine. However, based on these numerical benchmarks, we observe an $O(n \log^2 n)$ growth with ACA as well. LR Time in the legend is the time required to calculate the low-rank factorization.

solver perform much better than a conventional dense solver. As can be seen in Fig. 5(b), the solver is very accurate for $\epsilon_{ACA} = 10^{-10}$, which is the tolerance for which the speed results are obtained. Thus, the relative speed-up does not result in a significant loss of accuracy. One can observe that the ACA solver is faster than both the Chebyshev and Eigen solvers as a result of very low off-diagonal ranks. Figure 7 shows the factorization time, low-rank approximation time, solve time and total solve time separately for the ACA solver. Figure 8 shows the time vs matrix size (n). As can be seen both the fast solver with Chebyshev low-rank approximation and the fast solver with ACA low-rank approximation have asymptotic complexity of $\mathcal{O}(n \log^2(n))$.

7.2. Heat Transfer Problem in a 2D Turbine Blade Geometry

As mentioned in Section 6.1, we applied the fast solver algorithms to the top level frontal matrix of a 2D heat transfer problem in a turbine blade geometry. To this end, we compare two different approaches, namely, the fast direct solver algorithm (Section 4) with ACA low-rank approximation (Section 5.2) and the iterative solve algorithm (Section 3) with a BDLR (Section 5.3) direct solver as preconditioner.

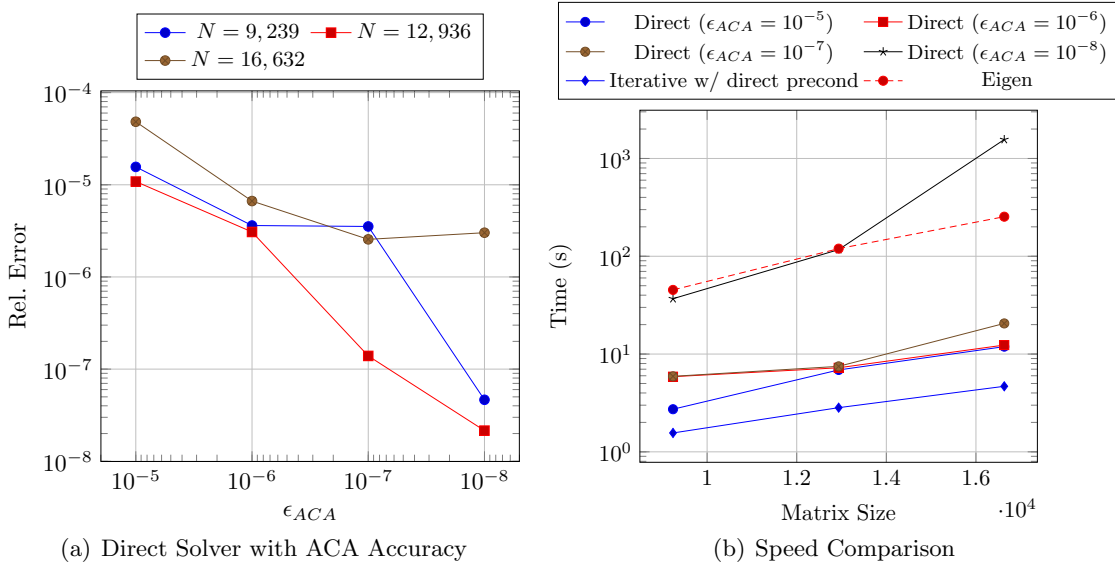


Figure 9: Application of the HODLR solver to the top frontal matrix of a turbine blade. a) ACA solver relative error vs. ACA tolerance (ϵ_{ACA}) for various matrix sizes. b) Speed comparison between ACA solver time vs. matrix size for various ACA tolerances (ϵ_{ACA}) and the direct/iterative solve method.

We should mention that for the direct solver with ACA approach, we used the pseudo-skeleton low-rank approximation scheme in combination with ACA. This is mainly because the ACA algorithm does not give accurate results in cases where interacting clusters have multiple points that are very close (e.g., the interaction between two halves of a closed curve). The pseudo-skeleton algorithm allows us to choose points more judiciously in the regions that are close to each other, and thus achieve a higher low-rank approximation accuracy. In such a case, we need to select more points near the boundary points of the curves in order to maintain accuracy and efficiency. For this, we have to construct a function that, given a set of indices $[i_a, i_b]$ and a desired number of indices r , outputs a set of indices $[i_1, i_r]$ such that a sufficient number of indices in the output sequence are located near i_a and i_b . The ‘‘Chebyshev’’ interpolation nodes provide such a functionality. Given an interval

$[a, b]$, the usual Chebyshev nodes in $[a, b]$ are located near a and b . Hence, in order to select the set of row indices, we consider the interval $[i_1, i_n]$. We then calculate the usual Chebyshev nodes in this interval, which are not integers. For each Chebyshev node x_k , we set the corresponding row index, i_k , to be the closest integer to x_k . The sequence of column indices is found in a similar manner. Although a heuristic, this approach has turned out to work well. This method can be viewed as a special case of the BDLR approximation scheme, which only works for 1D separators.

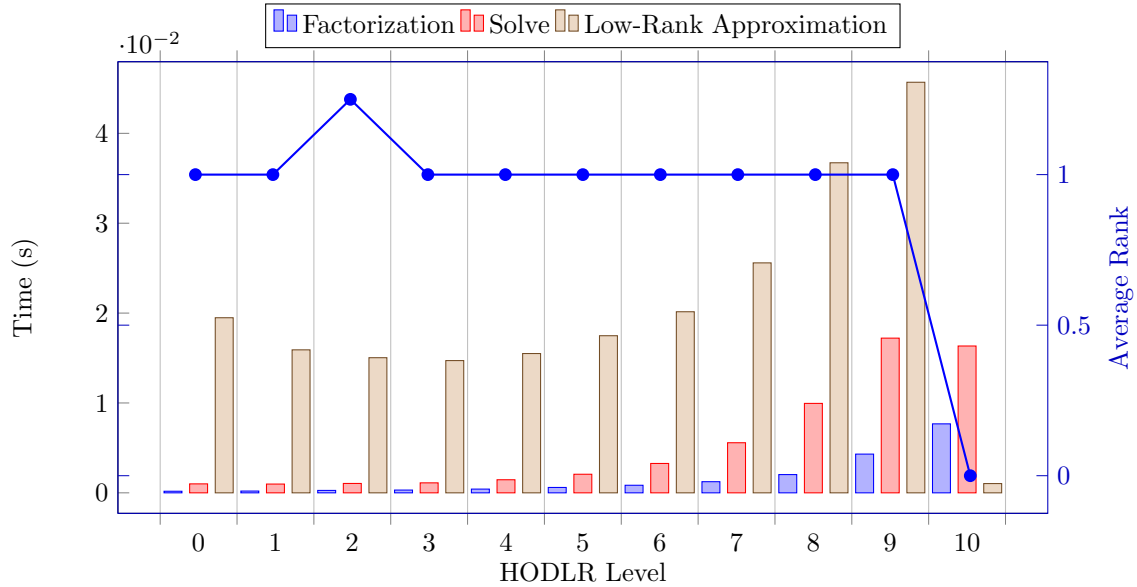
Figure 9(b) compares the speed of the direct solver with ACA low-rank approximation and the iterative solver (Section 3) with a fast BDLR direct solver as preconditioner. As can be seen, the iterative method is much faster than direct method with ACA. This is mainly because the BDLR method results in very low off-diagonal ranks (Figure 10(a)). Figure 9(a) shows the accuracy of the ACA solver as a function of tolerance. By comparing Figures 9(b) and 9(a), one can conclude that the ACA solver performs poorly for $\epsilon_{ACA} = 10^{-8}$. In this example, the ACA method is not a robust method for calculating the off-diagonal low-rank approximation. However, as seen in Figure 9(b) and Figure 10(b), the iterative solver with a fast BDLR direct solver as preconditioner, can reach machine accuracy much faster than the ACA and Eigen solvers.

7.3. Elasticity Equation for a 3D Beam

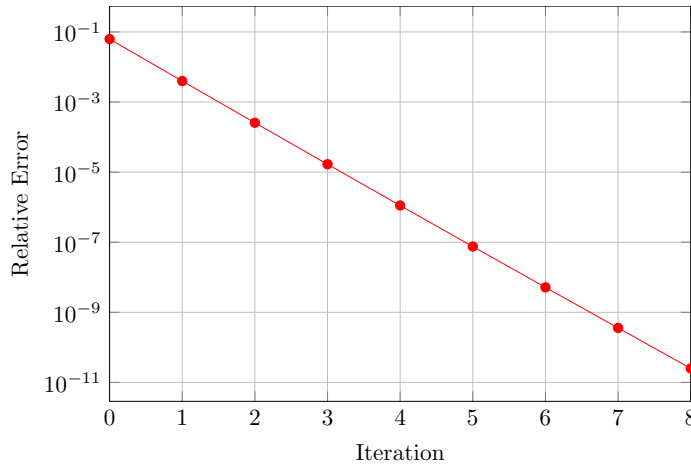
We investigated the application of the iterative solver with a fast BDLR direct solver preconditioner to frontal matrices arising from the multi-frontal elimination of a 3D elastostatics sparse matrix. As can be seen in Figure 3, the sparse matrix corresponds to an unstructured mesh. We have considered a mesh with approximately 300K degrees of freedom. Because of the particular geometry of the problem, all frontal matrices are relatively small ($\leq 2K$).

Figure 11 shows a detailed rank analysis of the top off-diagonal block of a sample frontal matrix. As can be seen in Figure 11(c), the singular values of the top off-diagonal block decay rapidly and the block is in fact low-rank. Figures 11(a) and 11(b) show the distance of row (column) index of each pivot obtained in the full pivoting LU factorization from the boundary between the row and column sets of vertices in the interaction graph. As we expected, larger pivots correspond to rows and columns that are closer to the boundary. Figure 11(d) compares the relative error in approximating the top off-diagonal block using SVD versus the BDLR approximation. That is, each point (x,y) in this plot represents the relative error in approximation (y) if we wanted a rank (x) approximation using one of the low-rank approximation algorithms. Needless to say, this corresponds to choosing the top singular values in the SVD decomposition and choosing rows and columns that are closest to the boundary in the BDLR approximation. One thing to note about this plot is that plots associated with the BDLR scheme have a tolerance (ϵ). This means that after the LU factorization of \hat{A} (see Section 5.3), we only keep rows and columns corresponding to pivots that are larger than ϵ times the magnitude of the largest pivot. We use this convention for all BDLR approximations in this paper. We can observe that as we decrease ϵ , we obtain a more accurate low-rank representation via the BDLR algorithm.

Figure 12 shows a detailed timing analysis of the iterative solver with a fast BDLR direct solver preconditioner applied to a sample frontal matrix. Figure 12(a) shows a level by level timing of the factorization, solve and low-rank approximation of the direct HODLR solver. Figure 12(b) shows the solve accuracy for each iteration.

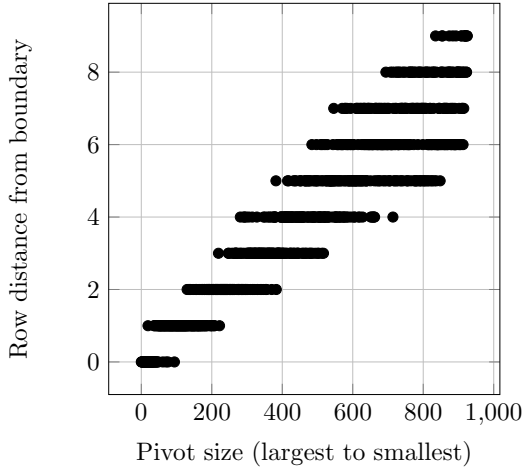


(a) Detail timings and rank information for direct HODLR solver

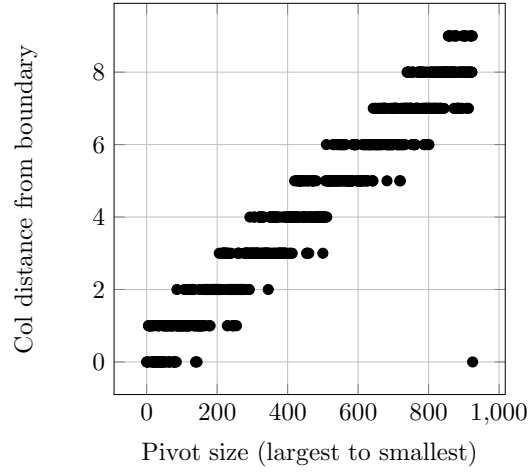


(b) Iteration accuracy

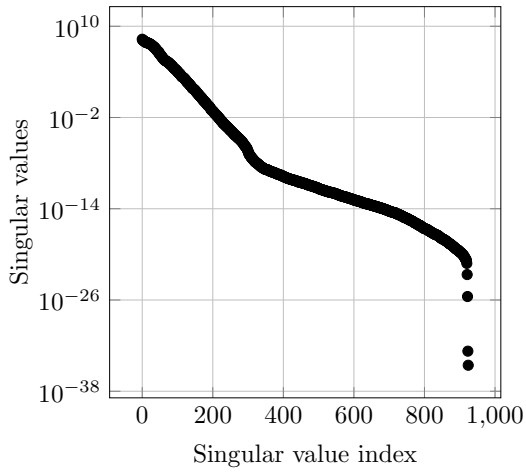
Figure 10: Figures are for the top level frontal matrix of a 2.14M stiffness matrix corresponding to an unstructured 2D mesh. The dense frontal matrix has a size of 16.6K. The pivot threshold for the direct solver is 0.1. That is, in obtaining the BDLR low-rank approximations, we only keep rows and columns that correspond to pivots that have a magnitude greater than 0.1 times the magnitude of the largest pivot. In computing the low-rank approximations, we only considered the vertices with distance at most one from the boundary. The average off-diagonal rank of each level in the HODLR tree is shown with bullets in figure (a). The numerical value of the rank can be read from the right y axis.



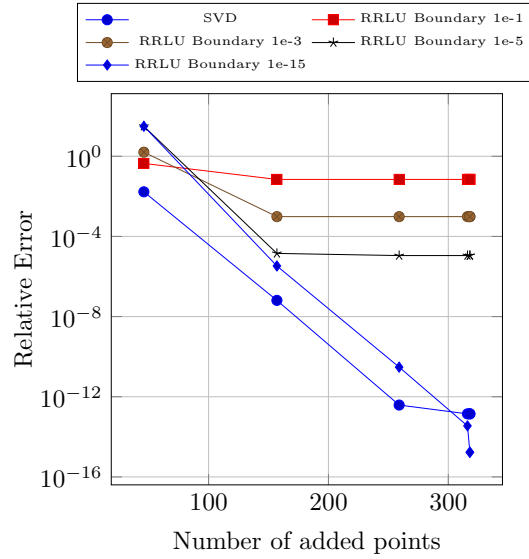
(a) Row distance from boundary vs pivot size



(b) Column distance from boundary vs pivot size

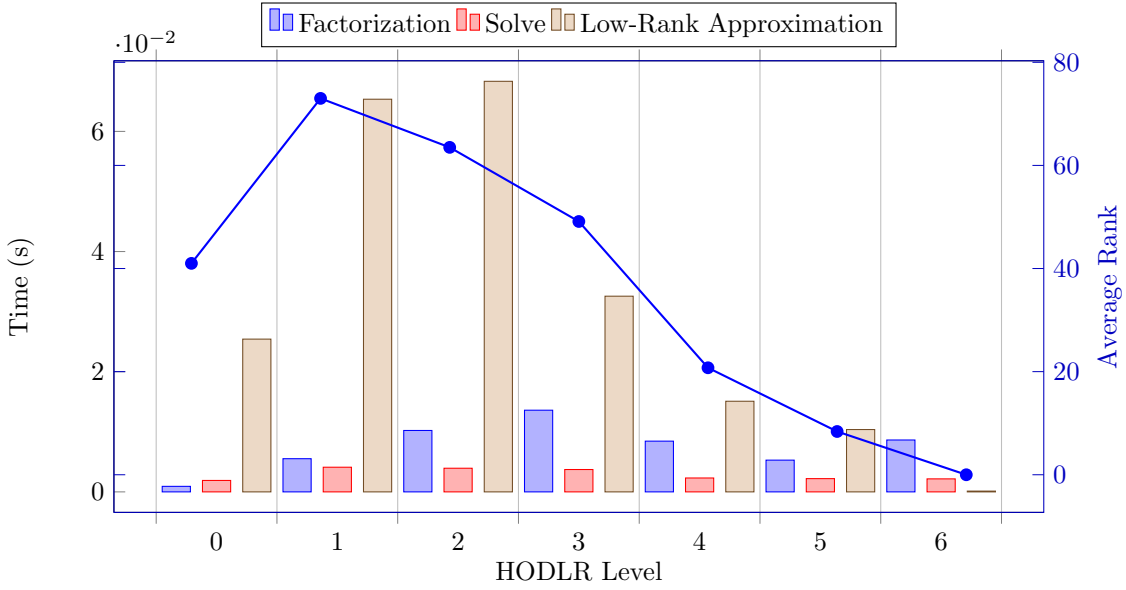


(c) Singular value decay

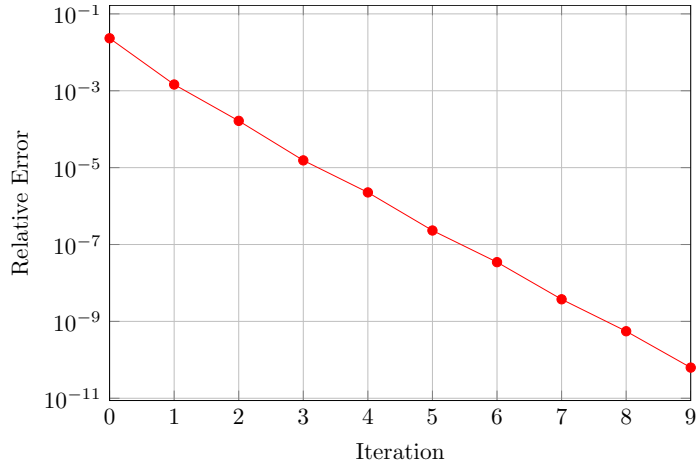


(d) Error vs number of added points

Figure 11: Figures are for the top off-diagonal block of a third level frontal matrix of a 300K stiffness matrix corresponding to an unstructured 3D mesh. The off diagonal matrix has a size of 1K.



(a) Detail timings and rank information for direct HODLR solver



(b) Iteration accuracy

Figure 12: Figures are for a third level frontal matrix of a 300K stiffness matrix corresponding to an unstructured 3D mesh. The dense frontal matrix has a size of 1.85K.

7.4. FETI-DP Solver for a 3D Elasticity Problem

We applied the iterative solver with BDLR direct solver preconditioner to frontal matrices arising from the multi-frontal elimination of local matrices in a FETI-DP solver. We considered two different class of problems. One corresponds to solving the elasticity equation (Eq. (28)) in a cube geometry with a structured mesh. The other corresponds to solving the same equation in an engine geometry with an unstructured mesh.

Figures 13 and 14 show a detail rank analysis of the top off-diagonal block of a frontal matrix of the structured and unstructured problem respectively. As can be seen in Figures 13(c) and 14(c), both off diagonal blocks are low-rank. Figures 13(d) and 14(d) show that the error in the BDLR method is comparable to the SVD (optimal) algorithm. Note that in Figure 13(d), the BDLR method with a tolerance of 10^{-15} has a higher relative error compared to higher tolerances for number of added points ≤ 400 . This is because the matrix \hat{A} (see Section 5.3) is actually low-rank and thus the LU factorization has very small pivots. These small pivots are the cause of the large relative error as they become very large when inverted.

Figures 15 and 16 show a detailed timing analysis of the iterative solver with a fast BDLR direct solver preconditioner applied to a sample frontal matrix of the structured and unstructured problem. Figures 15(a) and 16(a) show the detailed timings of the direct solver for both the engine and cube geometry respectively. Figures 15(b) and 16(b) show that the iterative solver with a fast BDLR direct solver preconditioner converges with a relatively low number of iterations in both cases.

7.5. Summary

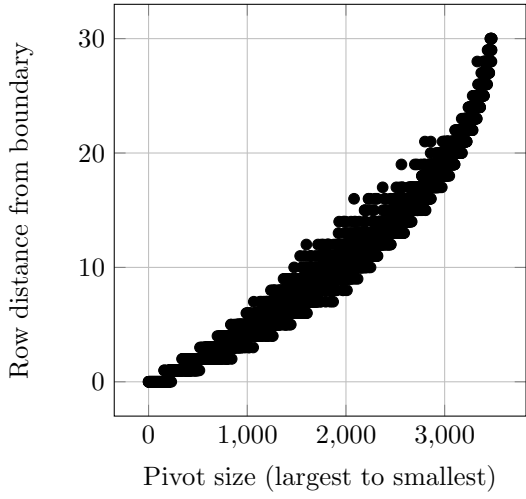
Table 3 summarizes the solver timings for various frontal matrices that we benchmarked. As can be seen, the iterative solve scheme with a fast BDLR direct solver preconditioner can reach machine accuracy much faster than a conventional LU solver in almost all cases. Further, as the matrix size increases, we see a more significant speed-up.

8. Conclusion and Future Work

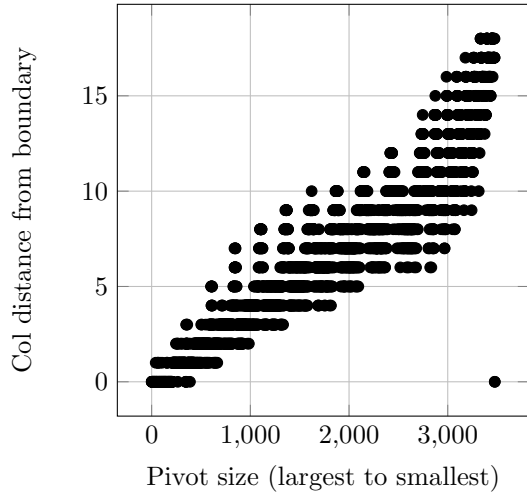
To reach our final goal of constructing a fast multi-frontal solver, we need to improve the slow dense solves for the frontal matrices, which we demonstrate through various benchmarks using the HODLR solver. It is also worth mentioning that using block low-rank structures like the HODLR structure will significantly reduce the memory consumption of a multi-frontal sparse solver. In practice, this is currently one of the main bottlenecks on existing hardware.

As explained previously, although the HSS structure leads to a faster factorization, it requires significantly more time to come up with the nested low-rank representation. In the end, HODLR may win the day because of the smaller computational time for finding the low-rank representation. This point is often skipped in many HSS papers. The simplicity of the HODLR+BDLR scheme, ease of implementation and parallel scalability provides an attractive framework to develop efficient direct solvers for finite element matrices.

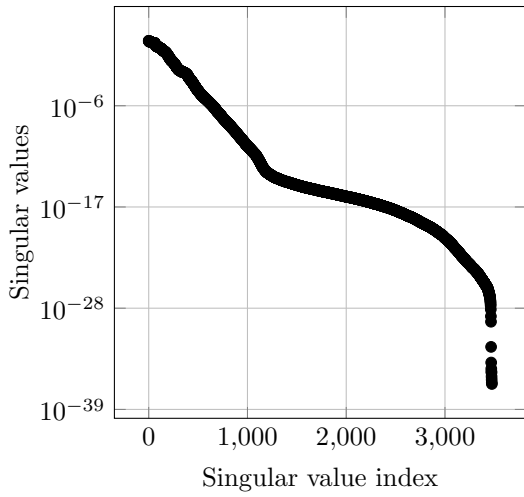
One of the major challenges in constructing a fast direct sparse solver is the need for a low-rank approximation scheme that works for algebraic Schur complements, as found in multi-frontal solvers. We have addressed this issue by introducing the BDLR low-rank approximation scheme which, as we've shown, is a very robust algorithm when applied to such matrices. In comparison, the ACA scheme gives poor results for such problems.



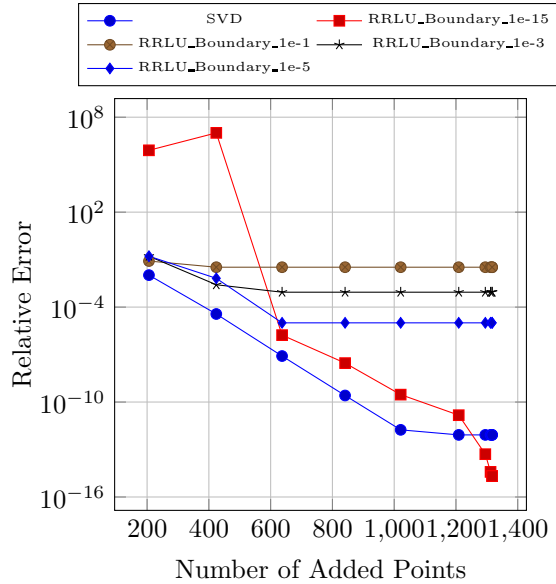
(a) Row distance from boundary vs pivot size



(b) Col distance from boundary vs pivot size

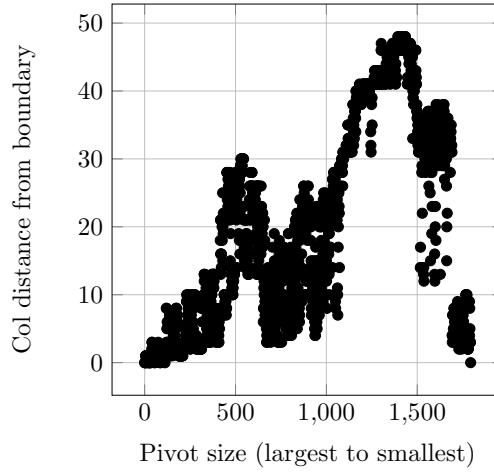
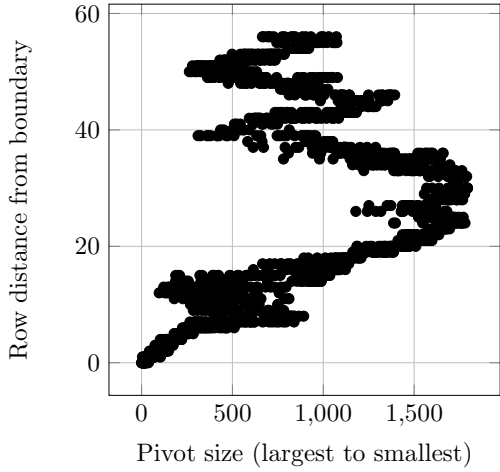


(c) Singular value decay



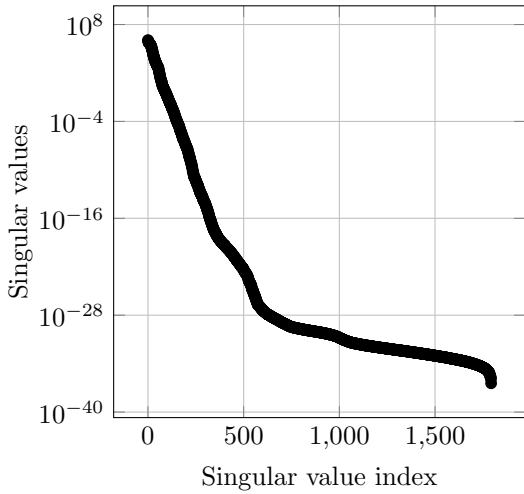
(d) Error vs NumPoints

Figure 13: Figures are for the top off-diagonal block of the top level frontal matrix of a 400K FETI local sparse matrix corresponding to a structured 3D mesh. The off diagonal matrix has a size of 3.5K.

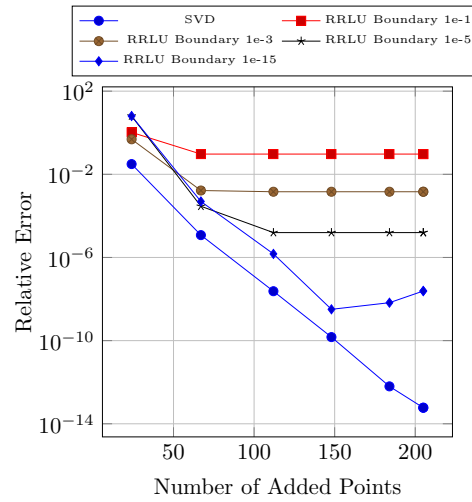


(a) Row distance from boundary vs pivot size

(b) Column distance from boundary vs pivot size

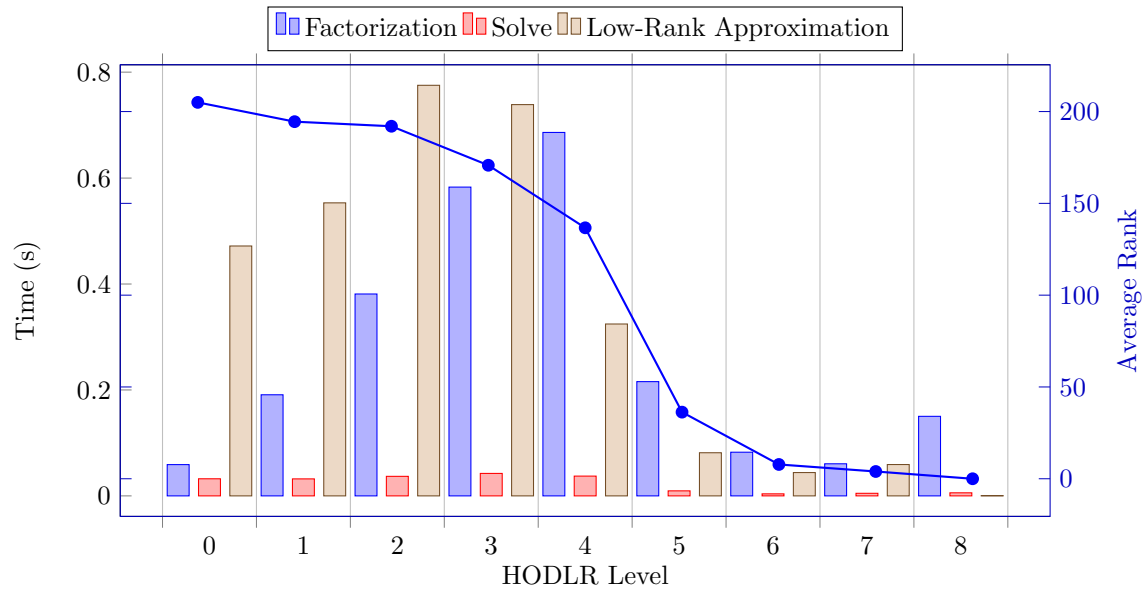


(c) Singular value decay

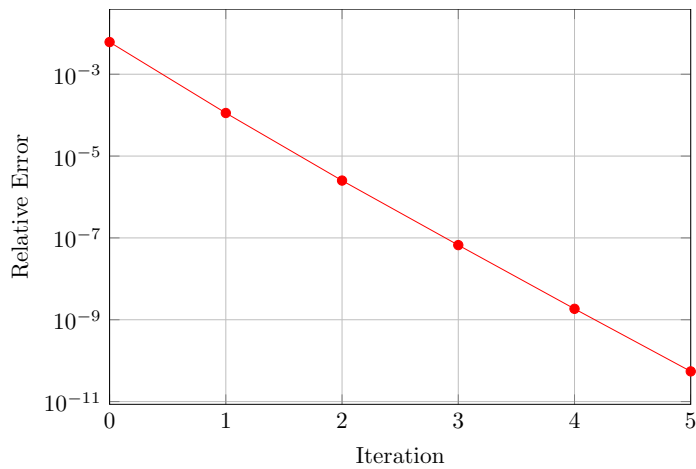


(d) Error vs NumPoints

Figure 14: Figures are for the top off-diagonal block of the 6th level frontal matrix of a 400K FETI local sparse matrix corresponding to an unstructured 3D mesh. The off diagonal matrix has a size of 1.8K.

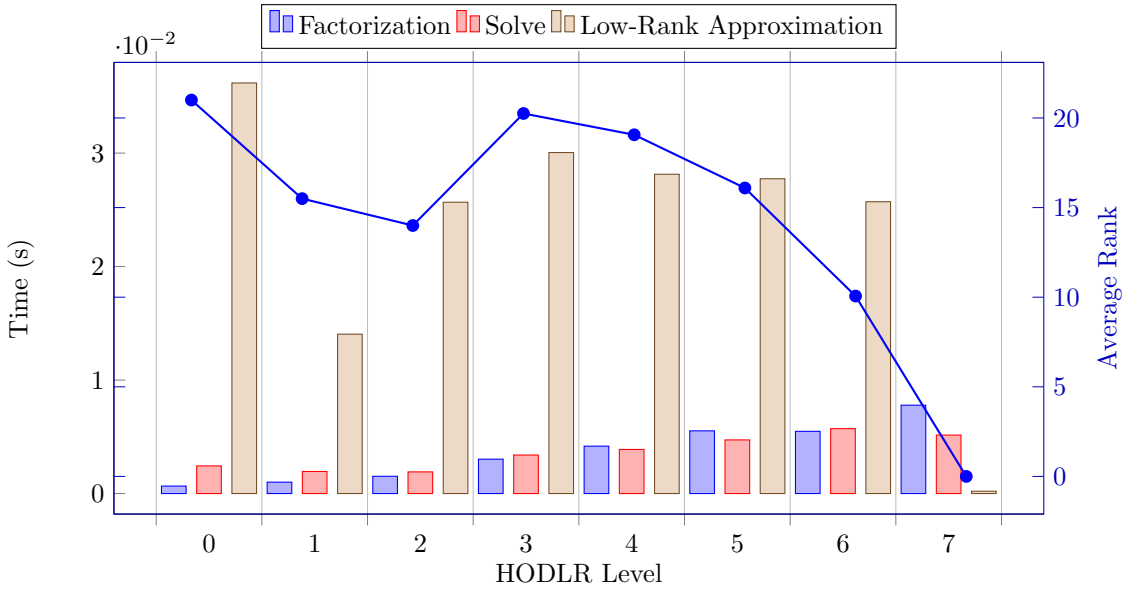


(a) Detail timings and rank information for direct HODLR solver

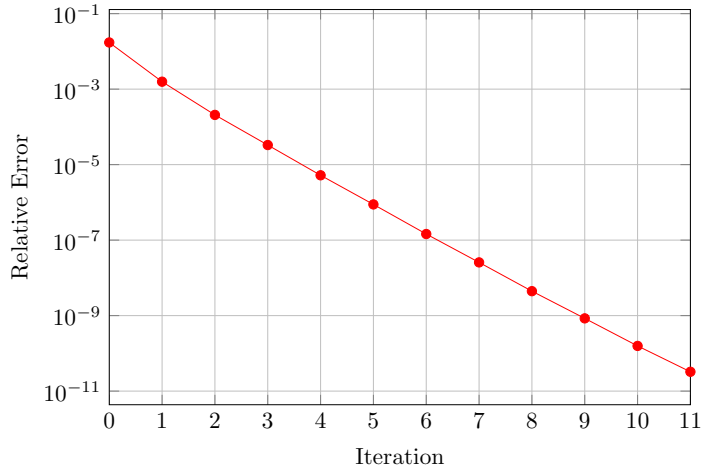


(b) Iteration accuracy

Figure 15: Figures are for the top level frontal matrix of a 400K FETI local sparse matrix corresponding to a structured 3D mesh. The dense frontal matrix has a size of 7K.



(a) Detail timings and rank information for direct HODLR solver



(b) Iteration accuracy

Figure 16: Figures are for the 6th level frontal matrix of a 400K FETI local sparse matrix corresponding to an unstructured 3D mesh. The dense frontal matrix has a size of 3.6K.

Matrix Type	Mesh Type	Mesh Dim	Level	Matrix Size		Direct Solver		Iterative Solver		I	LU	Speed-up
				Sparse	Dense	Time (s)	Accuracy	Time (s)	Accuracy		Time (s)	
FETI local	S	3D	3rd	400K	2.13K	3.80e-01	4.23e-03	4.47e-01	2.45e-13	7	5.83e-01	1.30
			3rd	400K	2.96K	9.25e-01	5.74e-03	1.23e+00	4.02e-12	13	1.48e+00	1.21
			3rd	400K	2.27K	3.18e-01	5.51e-03	4.09e-01	4.74e-12	8	7.37e-01	1.80
			2nd	400K	5.12K	2.39e+00	1.11e-02	2.93e+00	9.22e-13	8	7.60e+00	2.59
			2nd	400K	5.16K	3.16e+00	9.40e-03	3.75e+00	1.46e-12	8	7.46e+00	1.99
	1st	400K	6.94K	5.83e+00	6.29e-03	6.69e+00	1.63e-12	7	1.80e+01	2.69		
	Us	3D	13th	400K	2.06K	1.21e-01	3.15e-02	2.43e-01	9.57e-12	18	5.25e-01	2.16
			11th	400K	3.24K	2.13e-01	1.92e-02	5.38e-01	1.13e-11	15	1.93e+00	3.60
			7th	400K	2.36K	1.64e-01	2.97e-02	3.14e-01	1.31e-11	18	7.84e-01	2.50
			6th	400K	3.59K	2.28e-01	2.37e-02	5.28e-01	6.53e-12	13	2.60e+00	4.92
1st			400K	3.59K	2.28e-01	2.37e-02	5.28e-01	6.53e-12	13	2.60e+00	4.92	
stiffness	Us	2D	1st	1.26M	12.9K	1.84e-01	5.68e-02	2.84e+00	1.72e-12	10	1.13e+02	39.74
			1st	2.14M	16.6K	2.79e-01	6.23e-02	4.33e+00	1.64e-12	10	2.37e+02	54.77
			1st	642K	9.24K	1.26e-01	5.56e-02	1.55e+00	9.41e-13	10	4.20e+01	27.04
	Us	3D	3rd	300K	1.85K	2.83e-01	2.32e-02	3.55e-01	9.01e-12	11	3.84e-01	1.08
			3rd	300K	1.85K	2.96e-01	2.18e-02	3.80e-01	1.26e-11	13	3.98e-01	1.05
			3rd	300K	1.81K	2.40e-01	2.71e-02	3.23e-01	7.60e-12	14	3.72e-01	1.15
			3rd	300K	1.92K	2.80e-01	1.91e-02	3.66e-01	1.12e-11	13	4.21e-01	1.15
			2nd	300K	1.88K	2.77e-01	2.07e-02	3.40e-01	1.46e-12	10	4.19e-01	1.23
			2nd	300K	1.86K	2.81e-01	1.99e-02	3.53e-01	4.42e-12	11	3.92e-01	1.11
			1st	300K	1.84K	2.84e-01	1.82e-02	3.55e-01	5.66e-12	11	3.82e-01	1.08

Table 3: Summary of solver accuracy and speed for various benchmark cases. All timings are measured in seconds. Accuracy depicts the relative error in the solver solution. All LU timings are obtained using Eigen’s [34] partial pivoting LU solver. Column I shows the number of iterations required for convergence of the iterative solver for each case. Level indicates the level of the dense frontal matrix in the sparse elimination tree. Iterative solver time depicts total solve time for the iterative solver with a fast direct BDLR solver preconditioner (low-rank computation, direct solve, iteration, etc). ‘S’ refers to structured meshes and ‘Us’ refers to unstructured meshes.

One of the drawbacks of this method is that it relies on off-diagonal blocks being low-rank, which may not be true asymptotically as $N \rightarrow \infty$ for points distributed on a 2D or 3D manifold. More precisely, in 2D, the rank stays fairly constant but in 3D, there is a slow growth like $n^{1/2}$ where n is the size of the dense matrix or front. However, the HODLR scheme has a computational cost of $\mathcal{O}(r^2 n \log^2 n)$ with a relatively small constant in front of $r^2 n \log^2 n$. As a result, even if the rank r increases, the method stays competitive.

A major advantage of the mentioned direct solve algorithm is its parallel scalability. Since we make two independent recursive calls on each of the diagonal blocks, this method will scale very well. As a result, despite its somewhat higher number of flops (compared to an optimal $\mathcal{O}(n)$ method), the algorithm may run faster on large-scale parallel computers where communication and concurrency are key.

We estimate that the direct solver presented here starts being faster as soon as the rank r is $r \sim 0.4n$ compared to an $(2/3)n^3$ LU factorization algorithm. Recent work by Ambikasaran and Darve [2] has overcome the growth of rank in all dimensions by requiring a compression of well-separated clusters only. It is also worth mentioning that Ho and Ying [32] attempt to reduce the rank, when using interpolative decompositions to build low-rank approximations, with a scheme that reduces the dimensionality of the problem.

9. Acknowledgments

The authors would like to acknowledge Prof. Charbel Farhat and Dr. Philip Avery for providing us with the FETI test matrices. We also want to thank Prof. Pierre Ramet and Dr. Mathieu Favergue for their collaboration on this work.

Part of this research was done at Stanford University, and was supported in part by the U.S. Army Research Laboratory, through the Army High Performance Computing Research

Center, Cooperative Agreement W911NF-07-0027. This material is also based upon work supported by the Department of Energy National Nuclear Security Administration under Award Number DE-NA0002373-1.

References

- [1] Ambikasaran, S., 2013. Fast algorithms for dense numerical linear algebra and applications. Ph.D. thesis, Stanford University.
- [2] Ambikasaran, S., Darve, E., 2014. The inverse fast multipole method. arXiv preprint arXiv:1407.1572.
- [3] Ambikasaran, S., Darve, E. F., 2013. An $\mathcal{O}(N \log N)$ fast direct solver for partial hierarchically semi-separable matrices. *Journal of Scientific Computing* 57 (3), 477–501.
- [4] Ambikasaran, S., Foreman-Mackey, D., Greengard, L. F., Hogg, D. W., O’Neil, M., 2014. Fast direct methods for Gaussian processes and the analysis of NASA Kepler mission data. arXiv preprint arXiv:1403.6015.
- [5] Ambikasaran, S., Li, J. Y., Kitanidis, P. K., Darve, E. F., 2013. Large-scale stochastic linear inversion using hierarchical matrices. *Computational Geosciences* 17 (6), 913–927.
- [6] Ambikasaran, S., Saibaba, A. K., Darve, E. F., Kitanidis, P. K., 2013. Fast algorithms for Bayesian inversion. In: *Computational Challenges in the Geosciences*. Springer, pp. 101–142.
- [7] Bebendorf, M., 2000. Approximation of boundary element matrices. *Numerische Mathematik* 86 (4), 565–589.
- [8] Bebendorf, M., 2008. Hierarchical Matrices: A Means to Efficiently Solve Elliptic Boundary Value Problems. Vol. 63 of *Lecture Notes in Computational Science and Engineering (LNCSE)*. Springer-Verlag, ISBN 978-3-540-77146-3.
- [9] Benamou, J., Despres, B., 1997. A domain decomposition method for the Helmholtz equation and related optimal control problems. *Journal of Computational Physics* 136, 68–82.
- [10] Börm, S., Grasedyck, L., Hackbusch, W., 2003. Hierarchical matrices. *Lecture notes* 21.
- [11] Chandrasekaran, S., Dewilde, P., Gu, M., Lyons, W., Pals, T. P., 2006. A fast solver for HSS representations via sparse matrices. *SIAM Journal on Matrix Analysis and Applications* 29 (1), 67–81.
- [12] Chandrasekaran, S., Gu, M., Li, X., Xia, J., 2008. Some fast algorithms for hierarchially semiseparable matrices. Tech. rep., UCLA.
- [13] Chandrasekaran, S., Gu, M., Pals, T., 2006. A fast ULV decomposition solver for hierarchially semiseparable representations. *SIAM J. Matrix Anal.* 28 (3), 603–622.

- [14] Chen, J., 2014. Data structure and algorithms for recursively low-rank compressed matrices. Argonne National Laboratory.
- [15] Duff, I., Reid, J., 1983. The multifrontal solution of indefinite sparse symmetric linear equations. *ACM Transactions on Mathematical Software* 9 (3), 302–325.
- [16] Farhat, C., Lesoinne, M., LeTallec, P., Pierson, K., Rixen, D., 2001. FETI-DP: a dual-primal unified FETI method – Part 1: A faster alternative to the two-level FETI method. *International Journal for Numerical Methods in Engineering* 50, 1523–1544.
- [17] Fong, W., Darve, E., 2009. The black-box fast multipole method. *Journal of Computational Physics* 228, 8712–8725.
- [18] Gillman, A., Young, P., Martinsson, P., 2012. A direct solver with $O(N)$ complexity for integral equations on one-dimensional domains. *Frontiers of Mathematics in China* 7 (2), 217–247.
- [19] Goreinov, S., Tyrtyshnikov, E., Zamarashkin, N., 1997. A theory of pseudoskeleton approximations. *Linear Algebra and Its Applications* 261, 1–21.
- [20] Grasedyck, L., Hackbusch, W., 2003. Construction and arithmetics of \mathcal{H} -matrices. *Computing* 70 (4), 295–334.
- [21] Hackbusch, W., 1999. A sparse matrix arithmetic based on \mathcal{H} -matrices. Part I: Introduction to \mathcal{H} -matrices. *Computing* 62 (2), 89–108.
- [22] Hackbusch, W., Börm, S., 2002. Data-sparse approximation by adaptive \mathcal{H}^2 -matrices. *Computing* 69 (1), 1–35.
- [23] Hackbusch, W., Börm, S., 2002. \mathcal{H}^2 -matrix approximation of integral operators by interpolation. *Applied Numerical Mathematics* 43 (1), 129–143.
- [24] Hackbusch, W., Khoromskij, B., Sauter, S. A., 2000. On \mathcal{H}^2 -matrices. In: Bungartz, H.-J., Hoppe, R. H., Zenger, C. (Eds.), *Lectures on Applied Mathematics*. Springer Berlin Heidelberg, pp. 9–29.
- [25] Hackbusch, W., Khoromskij, B. N., 2000. A sparse \mathcal{H} -matrix arithmetic. *Computing* 64 (1), 21–47.
- [26] Hackbusch, W., Khoromskij, B. N., 2000. A sparse \mathcal{H} -matrix arithmetic: general complexity estimates. *Journal of Computational and Applied Mathematics* 125 (1), 479–501.
- [27] Hager, W. W., 1989. Updating the inverse of a matrix. *SIAM review* 31 (2), 221–239.
- [28] Han, J. C., Dutta, S., Ekkad, S., 2013. *Gas Turbine Heat Transfer and Cooling Technology*, second edition Edition. CRC Press.
- [29] Hecht, F., 2012. New development in freefem++. *Journal of Numerical Mathematics* 20 (3-4), 251–265.
- [30] Hestenes, M. R., Stiefel, E., 1952. Methods of conjugate gradients for solving linear systems. *Journal of Research of the National Bureau of Standards* 49 (6), 409–436.

- [31] Ho, K., Greengard, L., 2012. A fast direct solver for structured linear systems by recursive skeletonization. *SIAM J. Sci. Comput.* 34 (5), A2507–2532.
- [32] Ho, K., Ying, L., 2013. Hierarchical interpolative factorization for elliptic operators: integral equations. arXiv preprint arXiv:1307.2666.
- [33] Irons, B., 1970. A frontal solution program for finite element analysis. *International Journal for Numerical Methods in Engineering* 2, 5–32.
- [34] Jacob, B., 2010. Eigen v3. <http://eigen.tuxfamily.org>.
- [35] Kong, W., Bremer, J., Rokhlin, V., 2011. An adaptive fast direct solver for boundary integral equations in two dimensions. *Applied and Computational Harmonic Analysis* 31, 346–369.
- [36] Lai, J., Ambikasaran, S., Greengard, L. F., 2014. A fast direct solver for high frequency scattering from a large cavity in two dimensions. *SIAM Journal on Scientific and Statistical Computing*.
- [37] Li, J., O.Widlund, 2005. Feti-dp, bddc, and block cholesky methods. *International Journal for Numerical Methods in Engineering*.
- [38] Li, J. Y., Ambikasaran, S., Darve, E. F., Kitanidis, P. K., 2014. A Kalman filter powered by \mathcal{H}^2 -matrices for quasi-continuous data assimilation problems. *Water Resources Research*.
- [39] Liu, J., March 1992. The multifrontal method for sparse matrix solution theory and practice. *SIAM Review* 34 (1), 82–109.
- [40] Martinsson, P., 2009. A fast direct solver for a class of elliptic partial differential equations. *Journal of Scientific Computing* 38, 316–330.
- [41] Martinsson, P., Rokhlin, V., 2005. A fast direct solver for boundary integral equations in two dimensions. *Journal of Computational Physics*, 1–23.
- [42] Pellegrini, F., Roman, J., 1996. *SCOTCH*: A software package for static mapping by dual recursive bipartitioning of process and architecture graphs. *High-Performance Computing and Networking* 1067, 493–498.
- [43] Rjasanow, S., 2002. Adaptive cross approximation of dense matrices. In: *International Association for Boundary Element Methods Conference, IABEM*.
- [44] Saad, Y., Schultz, M. H., 1986. GMRES: A generalized minimal residual algorithm for solving nonsymmetric linear systems. *SIAM Journal on Scientific and Statistical Computing* 7 (3), 856–869.
- [45] Schmitz, P., Ying, L., 2012. A fast direct solver for elliptic problems on general meshes in 2D. *Journal of Computational Physics* 231, 1314–1338.
- [46] Wilson, D., Korakianitis, T., 1998. *The Design of High-Efficiency Turbomachinery and Gas Turbines*, second edition Edition. Prentice Hall.

- [47] Woolfe, F., Liberty, E., V.Rokhlin, Tygert, M., 2008. A fast randomized algorithm for the approximation of matrices. *Applied and Computational Harmonic Analysis* 25 (335-366).
- [48] Xia, J., Chandrasekaran, S., Gu, M., Li, X. S., 2009. Superfast multifrontal method for large structured linear systems of equations. *SIAM Journal on Matrix Analysis and Applications* 31 (3), 1382–1411.
- [49] Xia, J., Chandrasekaran, S., Gu, M., Li, X. S., 2010. Fast algorithms for hierarchially semiseparable matrices. *Numerical Linear Algebra with Applications* 17, 953–976.
- [50] Ying, L., 2009. Fast algorithms for boundary integral equations. In: *Multiscale Modeling and Simulation in Science*. Springer, pp. 139–193.